



Polymer workflow and troubleshooting

Introduction

Polymers and plastics are ubiquitous in the modern world, which means that producing them safely and efficiently takes on outsized importance from both an economic and an environmental viewpoint. Optimization of the polymer workflow could lead to improved better materials, cost savings, and ultimately less waste. Advanced analytical techniques like Fourier transform infrared (FTIR) and near-infrared (FT-NIR) spectroscopy play a crucial role in propelling the polymer workflow towards more optimal conditions.

This compendium looks at the way in which FTIR and FT-NIR can enhance polymer creation, troubleshooting, and failure analysis. In the section on polymer creation and aging, research is presented about the ways in which these techniques allow for monitoring of curing rates and processes. Highlighting the rapid feedback from FTIR, one article describes how the technique makes it possible to do time-based analysis of curing polyurethanes. Another tells how it can evaluate accelerated polymer aging through in situ measurements of the amount of carbon dioxide present in the sample.

A section of this compendium focuses on the use of spectroscopy to provide troubleshooting and failure analysis. The real-world benefits of this are obvious: Knowing why a part failed, determining whether a contaminant is present polymeric materials, or understanding how to obtain a representative sample from a bulk polymer product, will clearly help in navigating a competitive polymer industry. Individual articles about these aspects of the polymer workflow are included herein.

The rapid response and versatility of FTIR and FT-NIR spectroscopy make these non-destructive analytical techniques ideal for use in the polymer workflow, whether they are used for characterizing polymer components or monitoring production processes in real time. The collection of research papers and articles in this compendium highlights the advantages these modern analytical methods offer to the world of polymers.

Table of contents

Workflow	4
Propelling the polymer workflow	5
<hr/>	
Polymer creation and aging	6
In situ measurement of CO ₂ by FTIR for accelerated polymer aging evaluation	7
Time-based FT-IR analysis of curing of polyurethanes	11
Monitoring the UV cure process of a polymer based ink by FT-IR	14
Polymerization cure rates using FT-NIR spectroscopy	16
<hr/>	
Troubleshooting and failure analysis	20
Investigating why a plastic part failed	21
Polymer troubleshooting guide	25
Characterization of contaminants in recycled PET and HDPE using FTIR microscopy	28
Sampling considerations for the measurement of a UV stabilizer in polymer pellets using FT-NIR spectroscopy	33
<hr/>	

Workflow

Propelling the polymer workflow

From polymer development and production to plastics recycling

Thermo Fisher Scientific provides solutions to accelerate innovation and increase productivity throughout the polymer process. From the early stages of reaction processes through compounding, production, and even recycling, our instruments enable the characterization and quality control needed to ensure superior polymer products.



Learn more at thermofisher.com/polymeranalysis

Polymer creation and aging



***In situ* measurement of CO₂ by FTIR for accelerated polymer aging evaluation**

Authors

Jing Xu, Jessica Deng, and Rui Chen, PhD.,

Thermo Fisher Scientific

Introduction

Polymer aging refers to the degradation process that occurs in polymer materials over time when exposed to environmental stress factors such as heat, light, oxygen, moisture, and mechanical stress. These stressors lead to changes in polymers' physical and chemical properties, and ultimately affect their performance and durability. A thorough understanding of polymer aging provides insight to material lifetime, long-term stability, and durability. This aides in the design of materials with better resistance to aging as well as the development of accelerated aging tests for quality control and product certification.

To reduce the time needed to estimate the lifetime of materials, accelerated polymer aging studies focus on degradation chemistry to determine activation energies, thereby predicting degradation rates under normal use conditions. There are numerous accelerated aging methods for durability evaluation defined by the International Organization for Standardization (ISO). For examples, the ISO 4665 and ISO 4892 procedures utilize laboratory lamps to simulate external environments under sunlight (weathering). The ISO 2578 and ISO 11346 methods employ temperatures higher than those under actual use conditions. For accelerated aging studies within a short evaluation time, it is critically important to accelerate degradation using more than one type of stress factor.¹

Overall degradation kinetics can be tracked by monitoring changes in materials' physical properties and/or chemical properties. Fourier transform infrared spectroscopy (FTIR) has been extensively used in polymer aging studies, primarily for identifying oxidation products and quantifying oxidation extent.² Measurements of CO₂ evolution in polymer degradation have also been reported.³⁻⁷ Volatile gases, most commonly CO, CO₂ and H₂O, have been used to probe early-stage degradation where only low conversion or minor degradation levels are encountered.³ Gas evolution chemical pathways are intrinsic parts of the dominant degradation chemistry. For example, the oxidative degradation of polyethylene (PE) and polypropylene (PP) involves hydroperoxide intermediates, which are unstable to both heat and UV light, followed by alkoxy radicals and scission reactions to form carbonyl groups and end-alkyl radicals. Subsequent reaction of the end-alkyl radicals leads to the formation of CO₂.^{7,8} The rate of CO₂ generation directly correlates to the aging activation energy described by the Arrhenius equation (Equation 1), where k is the rate of CO₂ generation, A is the pre-exponential factor, E_a is the activation energy, R is the molar gas constant, and T is the absolute temperature.

$$k = Ae^{\frac{E_a}{RT}}$$

Equation 1.

In this application note, the quantitative determination of the aging activation energy for PP and PE, through the *in situ* FTIR measurements of CO₂ evolution inside an accelerated aging apparatus, is demonstrated.

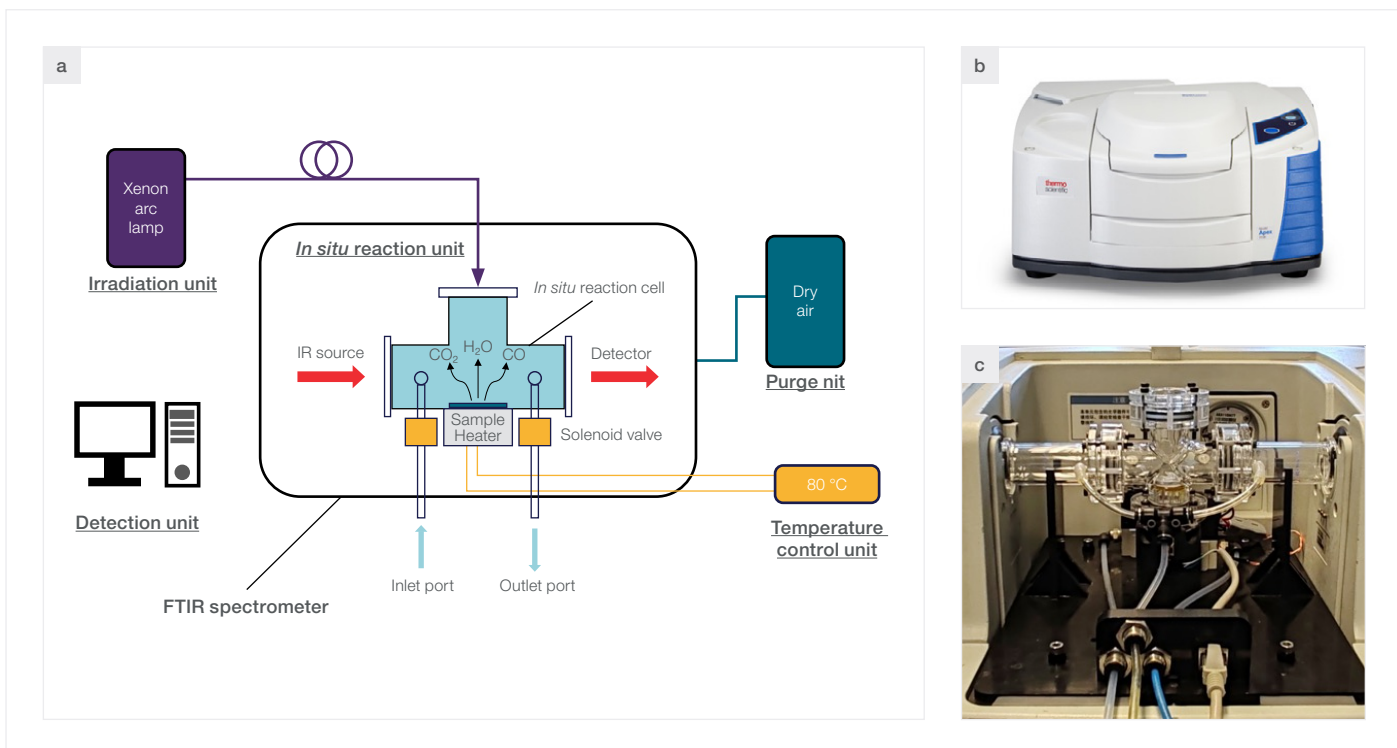


Figure 1. (a) The schematic illustrating the working principles of StabiEval-30 for accelerated aging studies; (b) photo of a Thermo Scientific™ Apex™ FTIR Spectrometer; and (c) photo of a StabiEval-30 apparatus inside the sample compartment of an Apex FTIR spectrometer.

Experimental

All experiments were performed using a Thermo Scientific™ Nicolet™ iS20 FTIR spectrometer, with an accelerated aging apparatus, StabiEval-30, placed in the main sample compartment (Figure 1). Note that since the experiments, the next-generation Thermo Scientific™ Nicolet™ Apex™ FTIR spectrometer (Figure 1b) was launched to succeed the iS20 FTIR spectrometer, with enhanced performance and a new software platform, Thermo Scientific™ OMNIC™ Paradigm Software, for data acquisition and analysis. The accelerated aging apparatus StabiEval-30 enables independent control of temperature, humidity, UV irradiation, and oxygen concentration, thus offering different combinations of these environmental factors to simulate different use conditions. The apparatus also serves as a gas cell that allows *in situ* measurements of the gases generated during degradation.⁹ The iS20 was equipped with a liquid nitrogen-cooled Mercury Cadmium Telluride (LN2-MCT) detector. Transmission mode was used for spectral collection with a spectral resolution of 4 cm⁻¹ and 32 scans were co-added for each spectrum. The Series function of the OMNIC software was used for data acquisition. The peak area of the spectra region 2,253-2,433 cm⁻¹ was used to track the CO₂ evolution.

Thin films of polymer samples were placed in the sample tray inside the StabiEval-30 reaction chamber. UV irradiation using a xenon lamp was maintained at 90 mW/cm² at 365 nm; the spectral distribution curve of the xenon lamp agrees well with that of sunlight. The apparatus was purged with dry air at a flow rate of 5 L/min for a minimum of 20 minutes prior to each aging test. The total duration of each accelerated aging test was 240 minutes and the FTIR measurements were taken at 5 minute intervals. For each test, the system was first equilibrated for 30 minutes (T-0 to T-30) until the FTIR background stabilized. The aging settings were then applied at T-30. The UV irradiation was shut off at T-210 and the data acquisition was stopped at T-240.

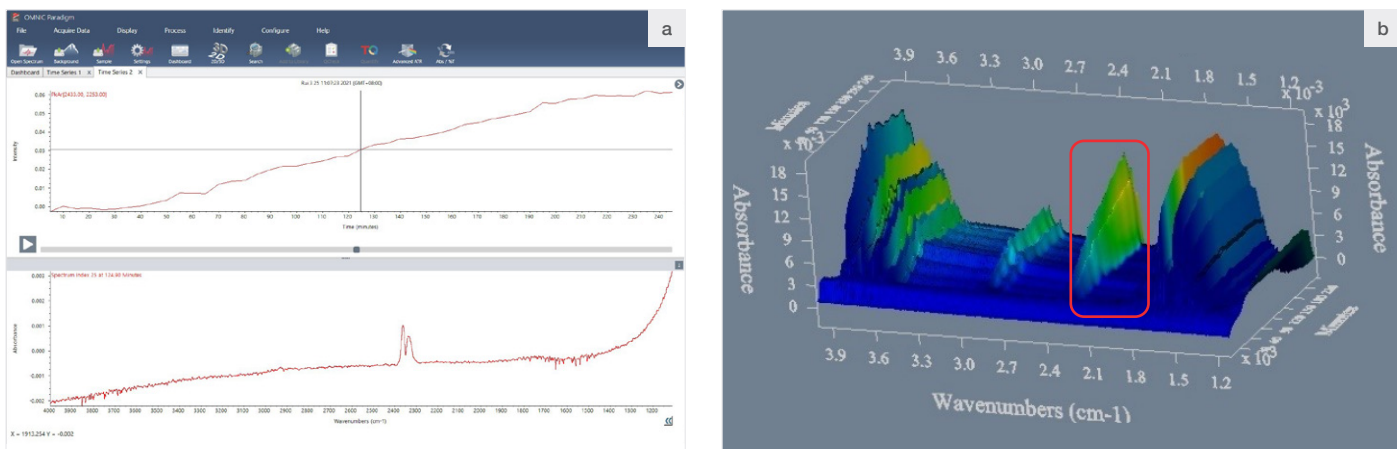


Figure 2. (a) Representative CO₂ peak area profile and FTIR spectrum of an accelerated ageing test; and (b) 3-D representation of an accelerated ageing test. The area inside the red rectangle shows the CO₂ evolution over the course of the experiment.

Results and Discussion

Figure 2a shows a representative peak area profile (top) constructed based on the peak area of CO₂ from the FTIR spectrum (bottom). Figure 2b is a 3-D representation depicting a complete aging experiment, in which the CO₂ evolution is highlighted in the red rectangle. At a quick glance, the CO₂ peak area increases steadily between T-30 and T-210 when the heating and UV irradiation were on. This rise portion of the peak area profile reflects the combined contributions from both photo- and thermo-oxidation. The profile plateaus after T-210 when the UV irradiation was turned off, suggesting that there is no appreciable CO₂ generated in the absence of UV light. Determination of the exact degradation pathways requires a more rigorous understanding of the materials under investigation and more controlled experiments; such testing is outside the scope of this application note. The observations here nonetheless highlight the synergistic impact of UV irradiation and heating on the overall oxo-degradation.

The results of the accelerated aging experiments for PP and PE at six different temperatures are summarized in Figures 3. These results demonstrate that (1) CO₂ was evolved from both PP and PE; (2) more CO₂ was evolved from PP than from PE; and (3) the rate of CO₂ generation, indicated by the slopes of the peak area profile between T-30 and T-210, increases as temperature increases. High temperatures impart thermal energy to polymer molecules, increasing their kinetic energy. This increased kinetic energy allows polymer chains to move more freely, making them more susceptible to bond breaking. At elevated temperatures, the combination of increased thermal energy and enhanced reactivity of polymer molecules leads to accelerated polymer degradation.

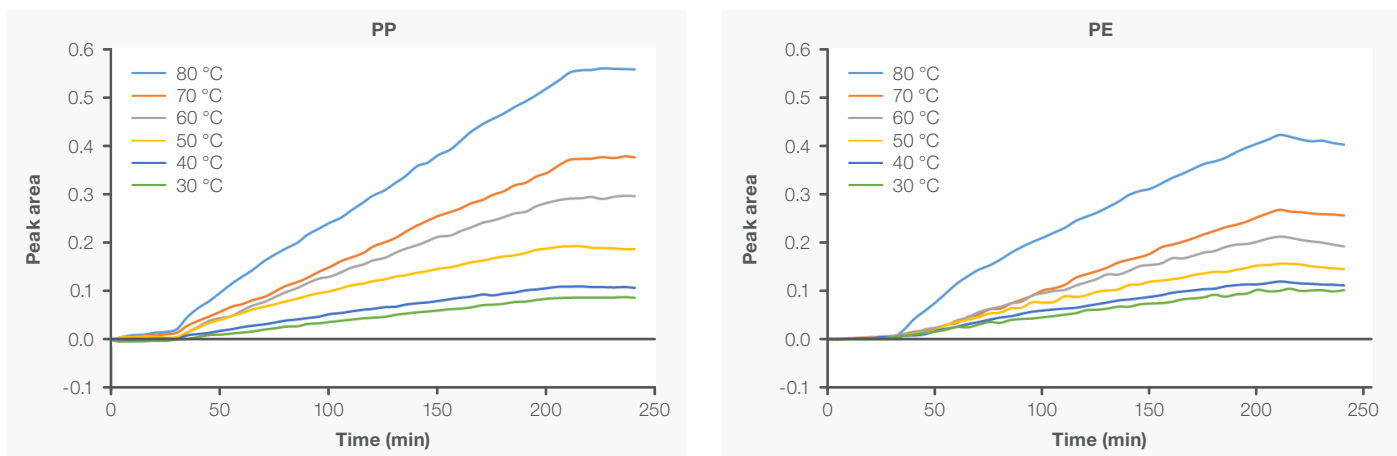


Figure 3. The CO₂ peak area profiles for PP and PE at six different temperatures.

Taking the natural logarithm of both sides of the Arrhenius equation (shown in Equation 1) leads to the following (Equation 2):

$$\ln k = \ln A - \frac{E_a}{RT} = -\frac{E_a}{R} \times \frac{1}{T} + \ln A$$

Equation 2.

There is a simple linear relationship between $\ln k$ and $\frac{1}{T}$. The slope of this linear relationship is $-\frac{E_a}{R}$, from which the Arrhenius activation energy E_a can be calculated. Figure 4 shows the Arrhenius plots ($\ln k$ vs. $\frac{1}{T}$) for PP and PE, with excellent linearity coefficients (R^2) in both cases. The calculated activation energies are 33 kJ/mol for PP and 25 kJ/mol for PE, respectively, with good agreements with the reported values in literature.¹⁰⁻¹¹ Note that the calculated activation energies here are largely phenomenological, because multiple reactions are occurring simultaneously. Caution should be exercised when interpreting and comparing the values.

Conclusions

In this application note, the *in situ* measurements of CO_2 evolution resulting from accelerated aging of PP and PE by FTIR, are described. The CO_2 evolution profiles at different temperatures exhibit Arrhenius behavior, from which the aging activation energies are calculated. The *in situ* measurements of CO_2 were enabled by a specially constructed gas cell that allows simultaneous UV irradiation, heating, and IR interrogation. FTIR shows great sensitivity in detecting trace level gaseous degradation products and is well suited to investigate early-stage polymer degradation. Each accelerated aging test was completed in less than five hours, much shorter than conventional accelerated tests. This experimental approach holds great promise in supplementing existing accelerated aging tests to better understand and evaluate aging behavior of a wide range of polymer materials.

References

1. Funabashi M., Ninomiya F, Oishi A, Ouchi A, Hagiwara H, Suda H, Kunioka M, *Journal of Polymers*, Volume 2016, Article ID 8547524.
2. X. Liu, C. Gao, P. Sangwan, L. Yu, Z. Tong, *J. Appl. Polym. Sci.* 2014, DOI: 10.1002/APP.40750
3. Giron, NH, Celina, *Polym Degrad Stab.*2017;145:93-101.
4. Christensen PA, Dilks A, Egerton TA, Temperley J. *J Mater Sci*, 1999;34:5689-5700.
5. Christensen PA, Dilks A, Egerton TA, Temperley J. *J Mater Sci*, 2000;35:5353-5358.
6. Christensen PA, Dilks A, Egerton TA, Lawson J, Temperley J. *J Mater Sci*, 2002;37:4901-4909.
7. C. Jin, P.A. Christensen, T.A. Egerton, E.J. Lawson, J.R. White, *Polym Degrad Stab.* 91 (2006), 1086-1096
8. Delprat P, Duteurtre X, Gardette J-L. *Polym Degrad Stab.*1995;50:1-12.
9. An Z., Yang R., *Acta Polymerica Sinica*, 2021,52(2):196-203. DOI:10.11777/j.issn1000-3304.2020.20150.
10. Cruz-Pinto JJC, Carvalho MES, Ferreira JFA, *Die Angewandte Makromolekulare Chemie*.1994, 216(1).113-133. DOI:10.1002/apmc.1994.052160108.
11. Jiri T, Zlata V. *Polymer Testing*. 2014, 36. 10.1016/j.polymertesting.2014.03.019.

Figure 4. The Arrhenius plot and the activation energy for PP and PE.

Time-based FT-IR analysis of curing of polyurethanes

Authors

Stefano Radice, Solvay Solexis, Milan, Italy

Mike Bradley, Ph.D.,
Thermo Fisher Scientific, Madison, WI, USA

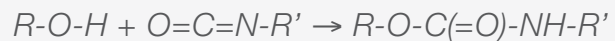
Keywords

- Adhesives
- Sealants
- Curing
- Series Software
- OMNIC Software
- Urethanes



Figure 1. Examples of items produced from polyurethanes. Photo of parts provided by Plastics International.

The polyurethane reaction starts with a diisocyanate (or a poly-isocyanate) reacting with a comonomer like an alcohol (frequently a diol):



Equation 1.

Thiols and amines can also be used (instead of the alcohol) – it is the reactivity of the acidic hydrogen which drives the reaction. This reaction can be very rapid, even at room temperature, so the liquid mixture rapidly becomes a solid. This rapidity can be used to produce unique products. For instance, during manufacturing, a little water can be added to the reaction mixture. The water reacts with the diisocyanate to produce a diamine and CO_2 . The CO_2 forms bubbles in the reaction mixture which are trapped within the rapidly forming polymer matrix, yielding polyurethane foam.

Shipping and storage of the liquid urethanes requires preventing the reaction (1) from occurring. This can be done by reacting the isocyanate with a “blocker”:



Equation 2.

where BH is the blocking agent. The blocking group can be eliminated at elevated temperatures, yielding the reactive isocyanate and initiating the cross-linking reaction. Different blocking agents will eliminate at different temperatures, so research into the best adapted blockers (least toxic, lowest deblocking temperature, etc.) is underway.

Introduction

The construction and automotive industries make use of a huge number of vendors, supplying anything from raw materials to complete assemblies. Among the critical components for both industries are adhesives and sealants. Each application requires specific characteristics, including curing conditions (temperature, moisture and speed of cure) and long term material properties, such as flexibility, UV resistance and bond strength.

The curing and working properties of adhesives generally result from polymerization reactions, which form a lattice of chemical bonds. Basic chemical kinetics identifies four steps in these polymerizations – initiation, propagation, termination and branching. The relative rates of these determine the properties of the final polymer. For instance, the termination step can control overall polymer chain length, branching impacts the cross-linking, and propagation rate determines curing times.

The initiation step is critical. Early initiation may result in ruined product, while sluggish initiation can lead to poor or slow curing. The initiation can be stimulated chemically, as in most two-part epoxies (the hardener stimulates a reaction in the resin), via UV-irradiation (many modern dental sealants) or using temperature. Storage needs require that the initiation reaction be halted until the proper moment. Urethanes provide an excellent example, where the initiation step can be blocked until heat is applied. Failing to do this can result in railroad cars filled with solid, useless, product.

A key part of investigating blocking agents requires studying the temperature dependence of the initiation and the time-evolution of the reaction mixture. Infrared is ideally suited to this, as the spectrum gives specific information regarding the progressing reaction. In the study highlighted here, FT-IR was able to elucidate both the progression and the mechanism for a crosslinking reaction.

Experimental

A Thermo Scientific™ Nicolet™ FT-IR spectrometer was used to collect infrared spectra at 15 second intervals, using 8 scans at 2 cm^{-1} resolution. The spectrometer was equipped with a KBr beam splitter and a DTGS detector. Our Thermo Scientific™ OMNIC™ spectroscopy software with the time-based Series™ software module was used to collect, process and present the data.

A perfluoropolyether diol (PFPE, Solvay Solexis) was mixed with ketoxime blocked isophorone diisocyanate (K-IPDI or IPDI once unblocked, Hüls-Degussa) in butyl acetate. This mixture was placed into a variable temperature cell, which was purged with dry air to remove volatiles during the reaction. The data reported here were obtained with an operating temperature of 150 °C.

Discussion

Table 1 gives the assignments for some of the observed infrared peaks.

Peak location (cm^{-1})	Chemical structure	Motion
3420-3200	N-H	Stretching
3000-2800	CH_2 and CH_3	Stretching
2260	NCO	Stretching
1740	C=O	Non-bonded urethane stretching
1690	C=O	Associated urethane and isocyanurate ring stretch
1510	H-N-C=O Amide II	Combined motion

Table 1. Assignment of major peaks, from references 1 and 2.

Figure 2 shows individual spectra taken at a series of time slices, and Figure 3 shows a large region of the dataset in the 3-D presentation of Series software. The 2260 cm^{-1} NCO peak can be seen to grow after initiation (as the blocker is removed), then disappear as the polymerization proceeds. The N-H blocking agent peak at 3420 cm^{-1} disappears rapidly. This is more clearly shown in the functional group time profiles in Figure 4.

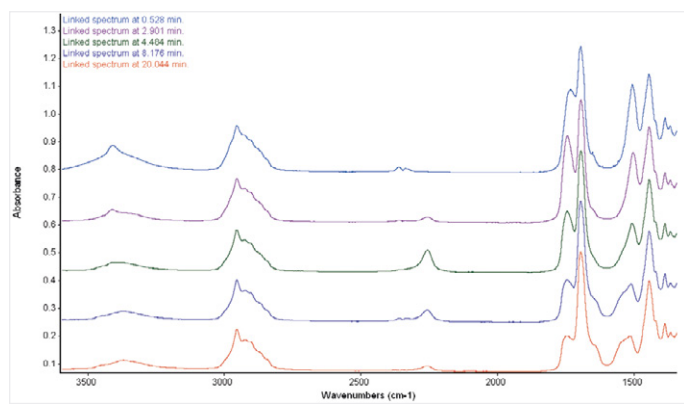


Figure 2. Time slices of spectra for the blocked urethane.

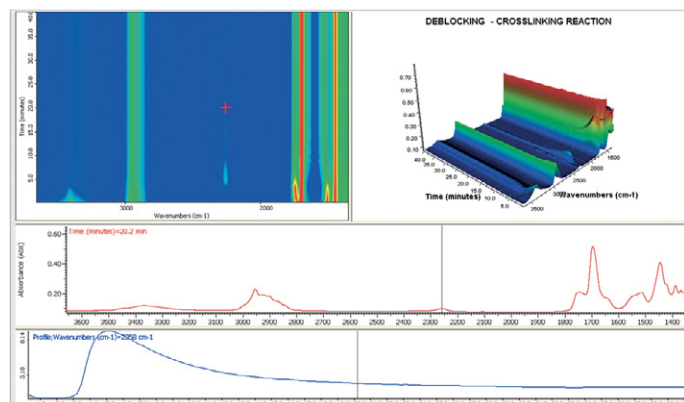


Figure 3. 3-D presentation of entire Series data set for the curing of the blocked urethane.

The intriguing aspect of this analysis is the insight into the reaction mechanism obtained from the profiles. Reactions (1) and (2) can occur sequentially (elimination (2) followed by addition(1)) or in a concerted manner (addition of the alcohol to the blocked isocyanate followed by elimination of the blocker). In the first case, the isocyanate intermediate would form immediately after the removal of the blocker, in the latter, the isocyanate would not form, or would form only later as thermally induced reversions of the urethane to the isocyanate. The data shown in Figures 3 and 4 supports the latter mechanism. The isocyanate does not form immediately upon unblocking, but shows a time delay consistent with thermal reversion of the urethane.

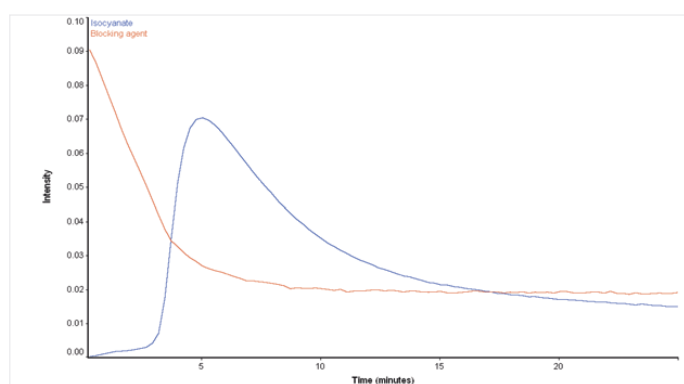


Figure 4. Time profiles of the intensity of the NCO and NH (blocking agent) during reaction.

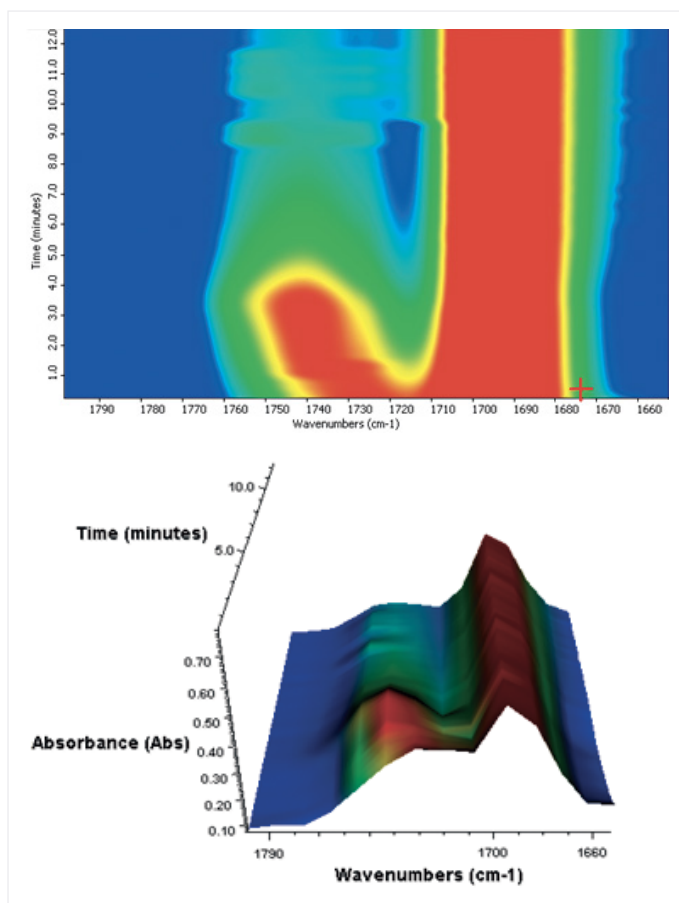


Figure 5. Contour and 3-D plot showing the shifting of the C=O peak as discussed in text.

Additional support for this mechanism is provided by the shift of the C=O band from 1734 to 1744 cm⁻¹. This is seen clearly in the contour and 3-D plots of a narrow region shown in Figure 5. The shift in the carbonyl peak is typical for urethanes close to fluorine.

Conclusion

The study of polymerization reactions requires the ability to take spectra against a time base under a wide range of conditions. The OMNIC Series software allows complete control over the experimental conditions, data collection parameters and starting trigger point. Further, the presentation capabilities provide excellent insights into subtle changes within the spectra.

Acknowledgement

The data was kindly provided by Solvay Solexis (solvaysolexis.com/). The analysis is largely based upon the discussion in the first reference.

References

1. Radice, S.; Turri, S.; Scicchitano M. *Applied Spectroscopy* 58(5), 2004, pp.535–542.
2. Turri, S.; Scicchitano, M; Marchetti, M.; Sanguineti, A.; Radice, S. in *Fluoropolymers 2: Properties*, (New York, Kluwer, 1999), p. 145.

Monitoring the UV cure process of a polymer based ink by FT-IR

Keywords

- FT-IR/polymers
- Inks
- Macros\Basic
- Paints & Pigments/ HATR/Quant
- Solid coatings

Introduction

The degree of cure of a polymer-based ink applied to a Mylar film is readily determined by FT-IR. The ink is screened onto the Mylar film and then exposed to UV light to cure the ink.

The determination of percent cure is an important quality control (QC) tool and may also be used to optimize the product manufacturing process.

Experimental

Spectra were collected using a Thermo Scientific™ Nicolet™ FT-IR spectrometer and a Smart Multi-Bounce horizontal ATR accessory with a zinc selenide crystal. The ATR sampling technique was chosen for this analysis to enhance the spectral response of the inked surface and to minimize the response of the bulk Mylar film base. The inked side of the Mylar film sample was simply pressed onto the surface of the ZnSe crystal of the ATR accessory. No sample preparation was required. Spectra were collected at 4 cm^{-1} with 32 sample scans (40 second sample collection time).

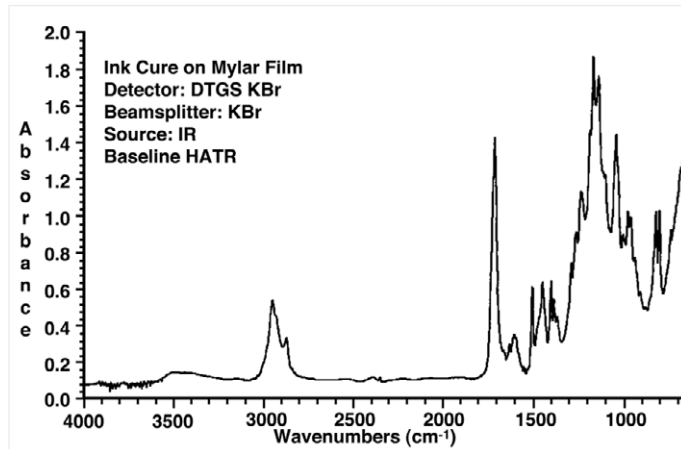


Figure 1.

Results

Figure 1 shows the spectrum of the sample prior to UV irradiation.

For this particular ink, the peak of interest is at 810 cm^{-1} and is related to free acrylate monomer. As the ink cures, there will be less of this free monomer, so the intensity of this peak will decrease. In order to quantify the degree of polymerization, an internal standard peak is needed. For this ink, the peak at 830 cm^{-1} is unrelated to the cure chemistry and remains unchanged. It is a simple exercise to monitor the ratio of these two peak heights in order to determine the amount of polymerization that has occurred during the cure process.

Figure 2 shows six spectra from the polymerization process with percent of cure ranging from 0 to 87%. Note that for these six spectra autoscaled on the 830 cm^{-1} absorbance, the band at 810 cm^{-1} varies in intensity. Where the peak heights of the 830 cm^{-1} and 810 cm^{-1} bands are nearly identical, the ink is uncured. Where the peak height of the 810 cm^{-1} band is lowest with respect to the 830 cm^{-1} absorbance the ink is 87% cured.

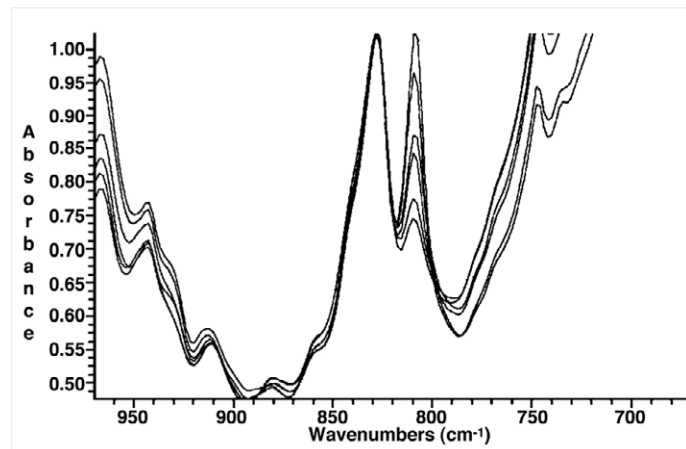


Figure 2.

Figure 3 shows a simple macro, written using Thermo Scientific™ OMNIC™ Macros\Basic™ software, that computes the ratioed peak height of $810\text{ cm}^{-1}/830\text{ cm}^{-1}$ for each sample spectrum using a base-line correction point at 895 cm^{-1} .

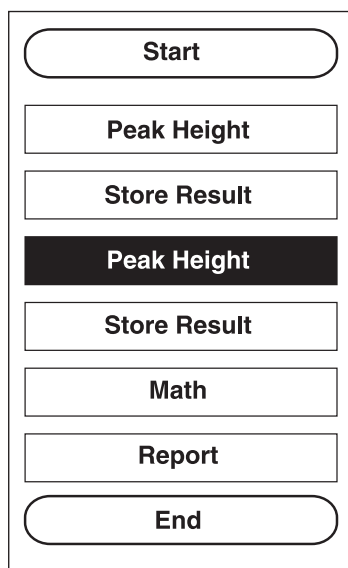


Figure 3.

The plot in Figure 4 shows a linear relationship between percent cure and the ratioed peak area. The physical properties of the cured ink are then related to the percent cure to determine the optimal manufacturing process for the UV cured ink based upon the QC determination of the spectral band ratios.

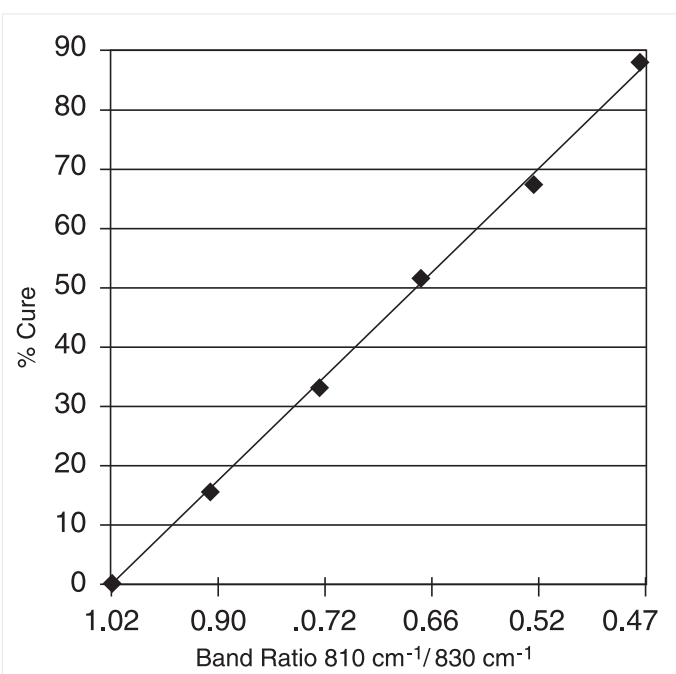


Figure 4.

Conclusion

The use of FT-IR with ATR sampling provides a fast and easy determination of the quality and state of UV curable polymerization in inks.

Polymerization cure rates using FT-NIR spectroscopy

Authors

Gabriela Budinova, PhD., Quintiles
GesmbH, Czech Republic, Europe
Ivor Dominak, PhD., NICODOM Ltd,
Czech Republic, Europe
Todd Strother, PhD.,
Thermo Fisher Scientific,
Madison, WI, USA

Keywords

Adhesive, Antaris, FT-NIR, kinetics,
polymerization, spectroscopy

Introduction

Rate of reaction is an important parameter in chemical processes. The speed of reactions and the extent of completion often govern the viability of certain processes and determine the suitability of these reactions for commercial purposes.

One area of particular interest lies with polymerization processes. Polymerization is the general term for processes that bind single chemical units into long chains. These long chains can also cross-link to form large networks of interlocking three-dimensional structures. Plastics, epoxy-type resins and various glues and adhesives are examples of materials that are formed through polymerization processes. Fourier transform near-infrared (FT-NIR) spectroscopy can be used to study reaction rates and is used here specifically to monitor polymerization of three types of commercially available adhesives.

Often polymers require two components: a monomer with a reactive center and a curing agent. The reactive center on the monomer may be an epoxy, alkene or alkyne, acrylate, carbonyl or other functional group. The curing agent initiates or catalyzes the polymerization process through cationic or anionic addition or some other free-radical mechanism. Three polymer adhesives were the subject of this study: 1) an epoxy resin, where the epoxy functional group on the monomer is bound to amines in the curing agent; 2) a methyl acrylate adhesive, where addition to the alkene functional group is catalyzed by a free radical initiator; and 3) a cyanoacrylate adhesive, containing a similar alkene functional group, but is instead catalyzed by the presence of water vapor in air.

Near-infrared spectroscopy takes advantage of the vibrational overtones and combination bands present in nearly all complex molecules. Light from an FT-NIR analyzer impinges on the sample, causing molecular vibrations at characteristic frequencies. The light is then collected by the analyzer and is displayed as spectra. Specific substances result in unique spectra that can be used for identification or quantification. For the current study, spectra of three polymer precursors were taken at various intervals during polymerization. Peak heights at specific frequencies were measured during the experiments as a demonstration of the analyzer's ability to monitor polymer cure rates.

Experimental

Sample 1: A two-component epoxy resin (Spolchemie, Czech Republic) was obtained and mixed according to the manufacturer's recommended protocol. Samples of the activated mix were collected and prepared for analysis with a Thermo Scientific™ Antaris™ II MDS FT-NIR (Figure 1). Spectra were collected for approximately 55 hours, during which the epoxy moieties were chemically altered by nucleophilic attack from the amines in the curing agent.



Figure 1. Antaris II MDS FT-NIR analyzer with integrating sphere (1a). The prepared samples were placed on top of the window over the integrating sphere, similar to what is shown in 1b, for the duration of the experiments.



Sample 2: A two-component acrylate base adhesive (UHU GmbH & Co, Bühl, Germany) was obtained from the manufacturer and mixed according to the recommended protocol. The transparent viscous acrylate copolymer contained a mixture of polymethylmethacrylate and methylmethacrylate monomers and was activated by free radicals generated from dibenzoylperoxide in the powdered curing agent. Samples of this acrylate-based adhesive were prepared for FT-NIR analysis as in sample 1. Spectra were collected for approximately 20 hours, during which the alkene functionalities disappeared through an additional mechanism.

Sample 3: A rapid-setting cyanoacrylate-based adhesive (Alteco, Osaka, Japan) undergoes anionic polymerization promoted by the presence of water vapor in air. As in sample 2, the carbon-carbon double bonds of the alkenes disappear as polymerization progresses. Samples of this material were analyzed with the Antaris FT-NIR without any preparation. While the reaction time is rapid, complete polymerization requires several hours, so the samples were analyzed for approximately 20 hours.

Data acquisition: The samples above were placed on a 0.5mm thick polyethylene film covering the integrating sphere. The signal contribution of the polyethylene film was ignored in the data analysis obtained from the samples. The samples were covered with aluminum foil to allow for beam reflection. Spectra were collected between 4000 and 10000 cm^{-1} ; scan resolution was set to 4 cm^{-1} and Norton-Beer apodization was used. The internal gold flag of the integrating sphere was used as the background. Simple baseline-corrected peak heights were measured at appropriate frequencies and monitored throughout the reactions.

Results and discussion

Sample 1: Figure 2a shows an overlay of spectra collected during the polymerization of the epoxy based resin in the region between 4488 – 4588 cm^{-1} . The absorption band at 4528 cm^{-1} associated with the epoxide group is shown to decrease in intensity throughout the data collection. The baseline-corrected peak height of the 4528 cm^{-1} band was plotted as a function of time (Figure 2b). The plot demonstrates that the peak height rapidly decreases in the first 1000 minutes (approximately 17 hours) essentially reaching its limit in approximately 2000 minutes (33 hours). This indicates that the reaction and curing process is complete in this time.

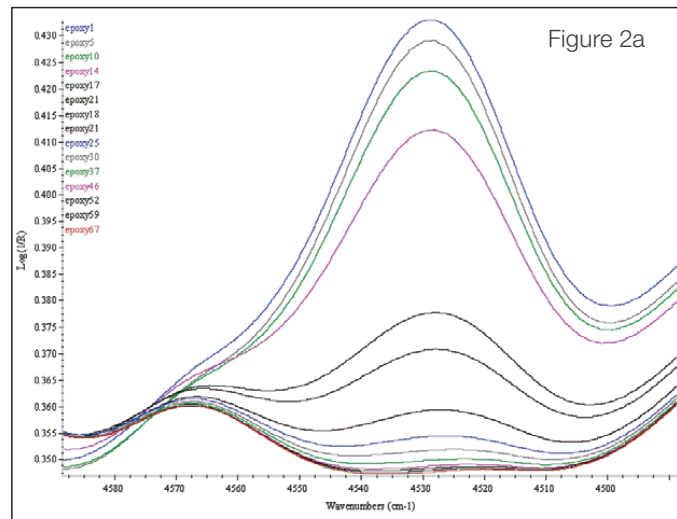
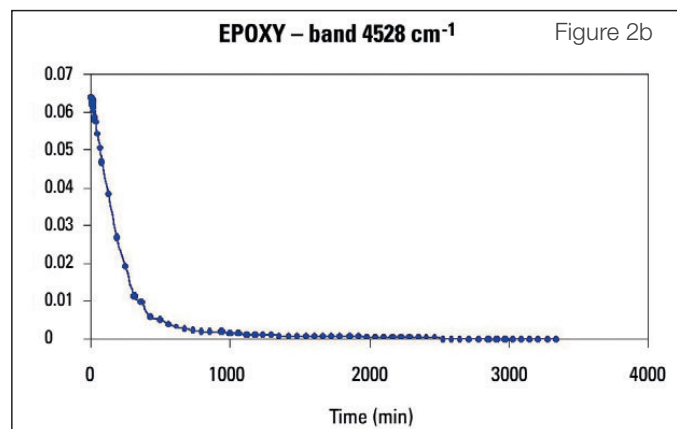


Figure 2a



EPOXY – band 4528 cm^{-1}

Figure 2b

Figure 2. Overlay of spectrum showing decrease in absorption band at 4528 cm^{-1} over time (2a). Plot of the baseline-corrected peak height as a function of time (2b). The peak clearly diminishes over time as the epoxide group disappears during the polymerization process.

Sample 2: Figure 3a shows the overlaid spectra between 6103 and 6234 cm⁻¹. Here the band at 6167 cm⁻¹ decreases as the polymerization progresses. This band is associated with the first overtone C-H stretch of an alkene. The baseline-corrected peak height of this band was also plotted as a function of time (Figure 3b). This plot shows a rapid decrease in peak height for the first 50 minutes, followed by a gradual decrease out to approximately 1200 minutes (20 hours). It should also be noted that the shape of the plot indicates there may be two or more chemical mechanisms accounting for the decrease in peak height.

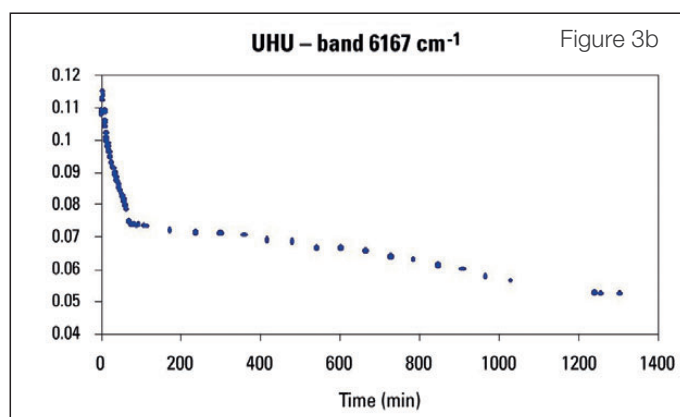
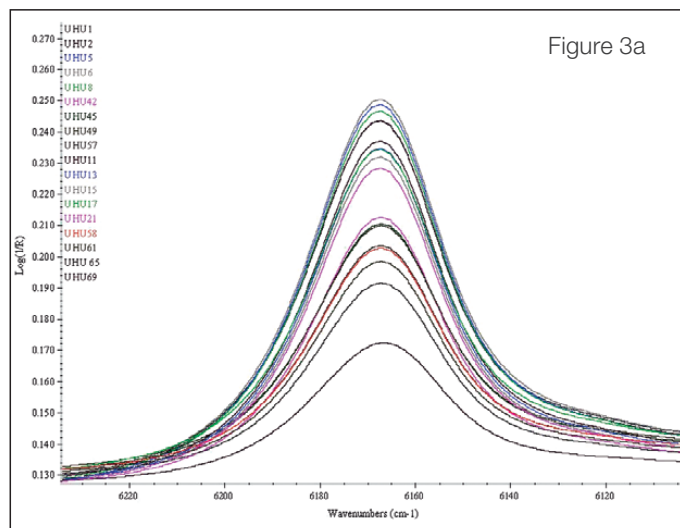


Figure 3. Overlay of spectrum in the range between 6103 and 6234 cm⁻¹ for acrylate-based adhesive showing a decrease in peak height over time (3a). Plot of the baseline-corrected peak height as a function of time (3b) indicates the loss of alkene groups is initially rapid, followed by a slower gradual decrease.

Sample 3: Figure 4a shows the overlaid spectra of one absorption band in the range between 4450 and 4590 cm⁻¹. As expected, the peak at 4495 cm⁻¹ diminishes as the polymerization progresses. Similar results were seen with bands at 4742 and 6208 cm⁻¹. The peak heights at 4495 cm⁻¹ were plotted over time (Figure 4b). The plot indicates that the polymerization rapidly occurred in the first few minutes and was essentially complete by 800 minutes (approximately 13 hours). This is expected behavior for this type of rapid-setting adhesive.

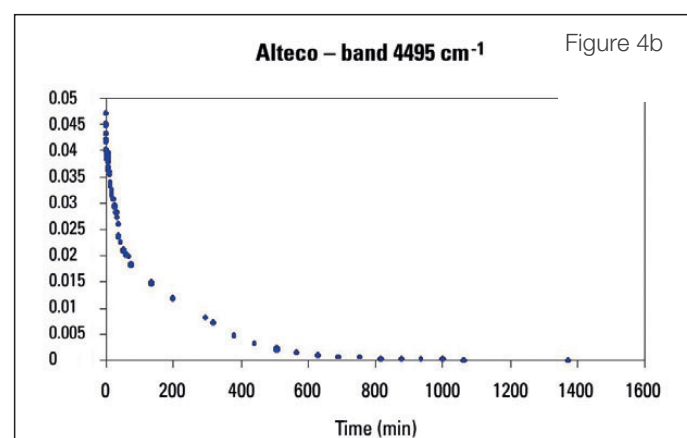
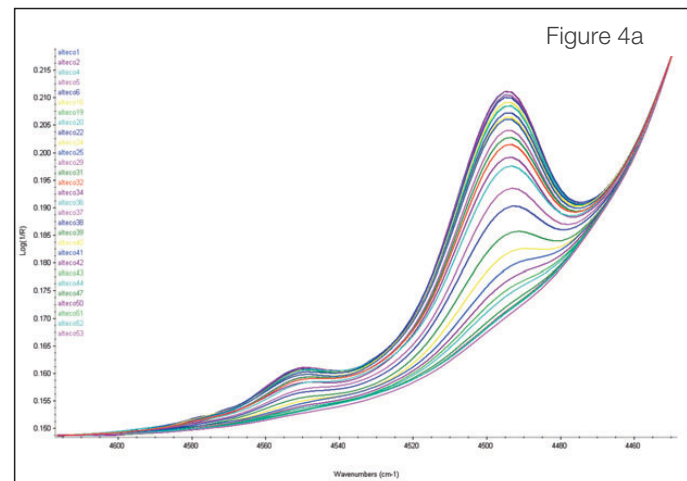


Figure 4. Overlay of spectrum in the range between 4450 and 4590 cm⁻¹ for rapid polymerizing cyanoacrylate adhesive (4a). Plot of the peak at 4495 cm⁻¹ as a function of time (4b) graphically demonstrates the rapid decrease in peak height associated with the rapid polymerization of this material.

Conclusion

The Antaris II FT-NIR analyzer was successfully used to monitor and track the chemical reaction rates of three polymerization reactions. An epoxy type polymer was shown to gradually cure with the loss of essentially all of the reactive groups by 2000 minutes. Polymerization of an acrylate-based adhesive was also monitored with the Antaris analyzer, with the reaction essentially complete within 1200 minutes. Finally, functional groups of a rapid-setting cyanoacrylate adhesive were shown to decrease as polymerization progressed, with the reaction essentially complete within 800 minutes. These examples clearly demonstrate the value of using the Antaris II FT-NIR analyzer to monitor reaction rates and observe reaction completion.

Troubleshooting and failure analysis

Investigating why a plastic part failed



Thermo Scientific Nicolet iS50
FTIR Spectrometer.

Keywords

ATR, diffuse transmission, failure analysis, FTIR, FT-Raman, polymer testing, spectroscopy

Abstract

Manufacturers employing plastic parts routinely face the challenge of analyzing failed parts to determine the root cause and corrective actions. The tools used to perform this analysis often include infrared and Raman spectroscopy for chemical composition, UV-Visible spectroscopy for color and optical transmissivity, and thermal analysis for determination of physical properties. This paper describes a study utilizing all of these tools to determine why a plastic part failed.

Introduction

A manufacturer of precision optical equipment designed a plastic cover for a device with specifications for chemical composition, surface texture, color and optical transmission. Briefly, the cover was to be made from a polycarbonate – acrylonitrile butadiene styrene (PC-ABS) blend with sufficient titanium dioxide to provide a slightly off-white color and optical transmissivity less than 0.01% T over a wide spectral range – from the UV into the near-infrared. The opacity was required to prevent ambient (room) light from entering the optical device and interfering with low light level measurements. Initially, all parts supplied met the specifications and the product provided satisfactory performance.

A re-engineering project was subsequently initiated to reduce costs and make the product more competitive. Alternate suppliers for various parts, including the cover, were asked for quotations. A new supplier underbid the original cover supplier, and the test parts met all the requirements for opacity. Production was shifted to incorporate this new supplier.

Shortly thereafter, the product began to fail critical performance tests. The failures were immediately traced to ambient light causing elevated backgrounds, strongly affecting low level optical measurements. Visual inspection of the covers did not reveal apparent differences from the original, but various control experiments led to tracing of the failure to the new cover. A root cause analysis using many techniques was undertaken to quickly identify and contain the issue.

Experimental results

UV-Visible spectroscopy

Diffuse transmission measurements of the original cover and failed cover were performed using a Thermo Scientific™ Evolution™ 220 UV-Visible Spectrophotometer and integrating sphere, displayed in Figure 1.

The cover by design contained significant quantities of particulates, which would efficiently scatter any transmitted light. For this reason, transmittance was measured with an integrating sphere. Pieces of covers from both good and failing devices were placed at the transmittance port of the sphere and spectra were collected from 220 to 800 nm, resulting in the spectra shown in Figure 2.



Figure 1. Evolution 220 UV-Visible Spectrophotometer (left), and sample compartment integrating sphere accessory (right).

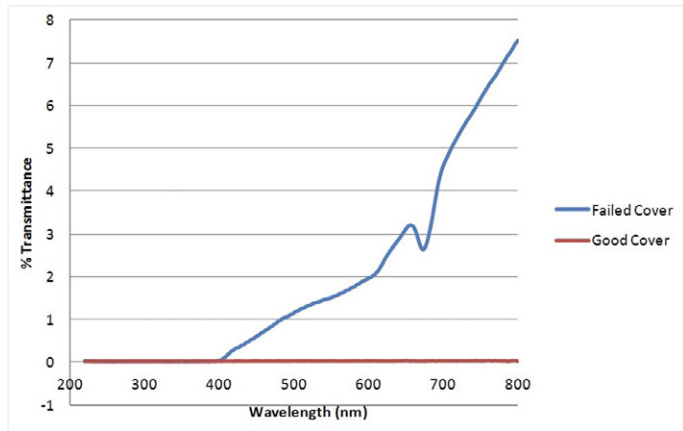


Figure 2. Diffuse Transmittance UV-Visible spectra of the failed cover (blue) and good cover (red), collected with an Evolution 220 UV-Visible Spectrophotometer and integrating sphere accessory.

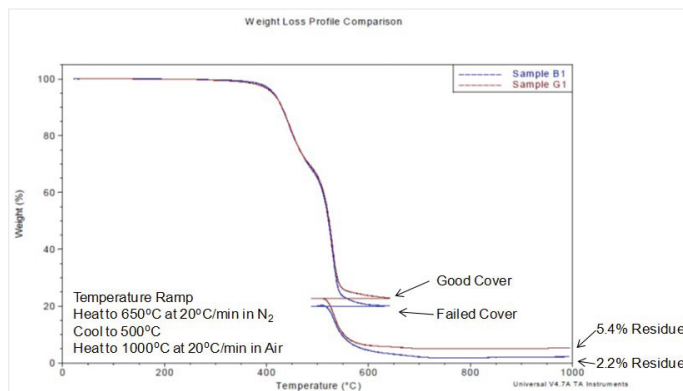


Figure 3. Thermogravimetric analysis weight loss curves for the good cover (red) and failed cover (blue), showing that the good cover has significantly higher inorganic content than the failed cover.

Essentially no transmittance was measurable through the good cover. In contrast, a significant transmittance through the visible part of the spectrum, greater than 7% T, was measured from the failing cover. This clearly explained the poor performance – the light leak – of the device under ambient conditions, but did not identify the root cause.

Thermogravimetric analysis (TGA)

Small pieces of the two covers were then measured with a TA Instruments™ thermogravimetric analyzer to determine bulk composition, with results shown in Figure 3.¹ The samples were heated from ambient to 650 °C at 20 °C/min under N₂ purge, then cooled to 550 °C, and heated again to 1000 °C at 20 °C/min with air purge.

The initial heating ramp under nitrogen pyrolyzes the organic component of the covers, and the final temperature ramp in air burns the remaining organic components leaving only oxides of the inorganic content.

The organic decomposition profiles of the two covers were nearly identical, indicating that both had the same plastic composition. However, the good cover had residual inorganic component representing 5.4% by weight, while the failed cover had an inorganic component of only 2.2% by weight. This indicated a significant difference in the inorganic filler amounts between the covers and provided a strong clue as to the source of the light leak.

Infrared analysis

Infrared spectra of small pieces of the two covers were collected using the integrated diamond iS50 ATR on a Thermo Scientific™ Nicolet™ iS50 FTIR Spectrometer, as shown in Figure 4. The built-in iS50 ATR on the Nicolet iS50 has a dedicated detector which permits the collection of combined mid- and far-IR ATR spectra down to 100 cm⁻¹. The ability of the iS50 ATR to collect spectra in the far-IR allows easy measurement and identification of inorganic fillers in plastic parts.



Figure 4. Nicolet iS50 FT-IR spectrometer with built-in diamond iS50 ATR, iS50 ABX Automated Beamsplitter exchanger, and sample compartment iS50 Raman accessory.

When combined with the iS50 ABX Automated Beamsplitter exchanger on the Nicolet iS50 Spectrometer, mid and far-IR spectra can be automatically collected and stitched together using a Thermo Scientific™ OMNIC™ Macros\Pro™ Visual Basic Program to provide a single spectrum of a sample from 4000 to 100 cm^{-1} .²

The ATR spectra of the plastic parts, shown in Figure 5, were corrected using the advanced ATR correction algorithm³ in Thermo Scientific OMNIC Software. The advanced ATR correction algorithm accounts for both relative intensity changes caused by sample penetration depth as a function of wavelength and also for peak shifts in the infrared spectra due to index of refraction differences between the ATR crystal and sample. Inspection of the infrared spectra of the two plastic pieces shows the polymer composition to be similar, but the original plastic part has an elevated baseline below 800 cm^{-1} , and a sharp peak at 360 cm^{-1} , as shown in Figure 6, that are absent or very weak in the spectrum of the replacement part. The peak at 360 cm^{-1} is below the range of a typical mid-IR spectrometer equipped with a KBr beamsplitter. The iS50 ABX with a solid substrate far-IR beamsplitter makes the far-IR range accessible in this analysis, while maintaining no compromise high performance across the entire range.

There are additional differences between the spectra which are emphasized through a spectral subtraction. The difference spectrum (Figure 5, bottom) shows small peak shifts in the polymer bands, indicating a small polymer composition difference between the two parts, typical when comparing plastic parts made by different suppliers, but a significant spectral difference is also observed below 800 cm^{-1} .

A library search of the difference spectrum against a forensic library of automobile paint pigments and fillers,⁴ shown in Figure 7, matches rutile, one of the crystalline forms of titanium dioxide, indicating a formulation difference between the two covers.

FT-Raman analysis

To confirm the conclusions drawn from the infrared analysis, the two samples were also analyzed using the iS50 Raman sample compartment FT-Raman accessory on the Nicolet iS50 Spectrometer (shown in Figure 4). The iS50 Raman accessory snaps into the sample compartment of the Nicolet iS50 FTIR Spectrometer, not requiring an external module typical of other FTIR spectrometer systems. The iS50 Raman accessory permits easy collection of Raman spectra with a near-infrared beamsplitter and InGaAs detector mounted inside the spectrometer.

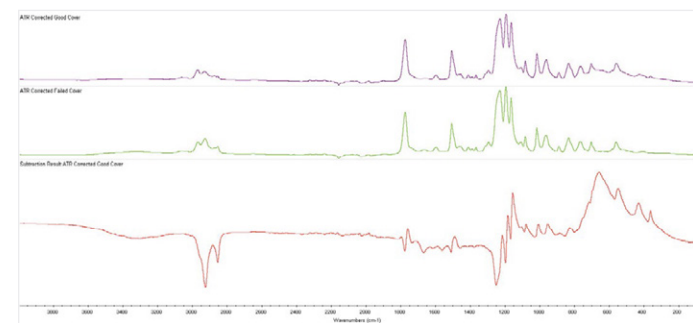


Figure 5. Advance ATR corrected infrared ATR spectra of the good plastic cover (top), failed plastic cover (middle) and difference spectra between the two (bottom).

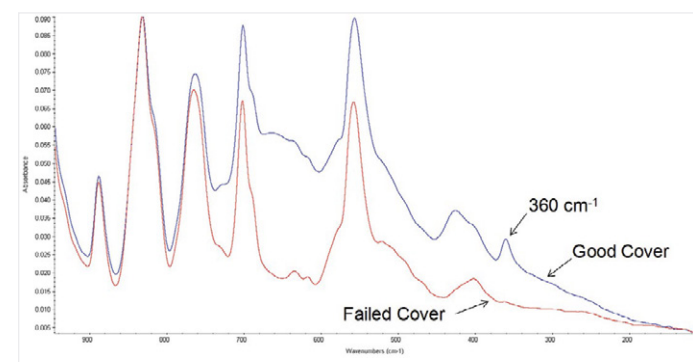


Figure 6. Overlay of the advanced ATR corrected spectra of the good cover (blue) and failed cover (red), over the spectral region from 940 to 100 cm^{-1} . Note the elevated baseline and the absorbance band at 360 cm^{-1} in the spectrum of the good cover that are absent or highly reduced in the spectrum of the failed cover.

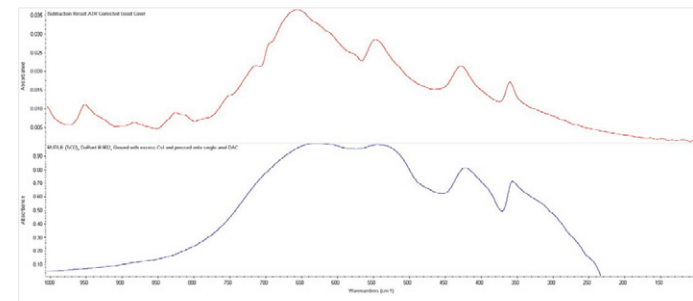


Figure 7. FT-Raman difference spectrum between the good and failed covers (blue), and top match from a library search against a forensic automobile paint pigment and fillers library (red), identifying a higher concentration of rutile (titanium dioxide) in the good cover.

FT-Raman spectra of the good and failed covers, along with the spectral difference spectrum between them, are displayed in Figure 8. FT-Raman spectroscopy allows collection of spectra into the far-IR region, complementing the capability of the Nicolet iS50 FTIR Spectrometer with the built-in iS50 ATR and ABX gaining access to this region. Again, the two spectra are very similar, demonstrating similar polymer composition, with small differences in the spectra observable below 800 cm^{-1} , clearly seen in the difference spectrum.

A library search of the difference spectrum against a minerals Raman library⁵ is displayed in Figure 9, identifying the difference between the two plastic parts as rutile, confirming the identification from infrared analysis.

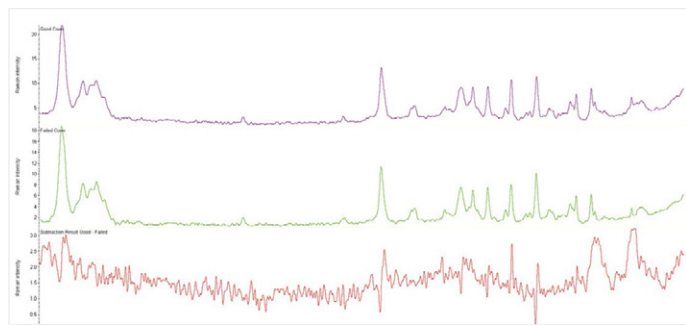


Figure 8. FT-Raman spectra of the good cover (top), failed cover (middle), and subtraction result between the two (bottom).

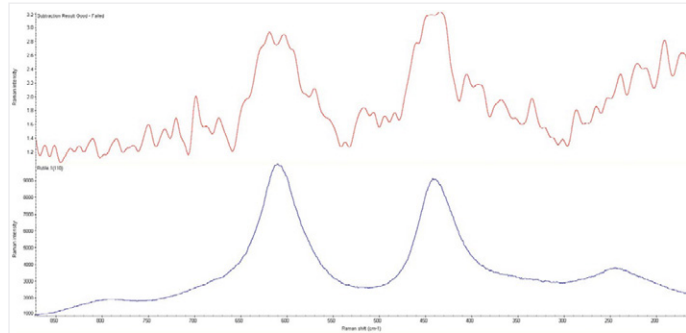


Figure 10. FT-Raman difference spectrum between the good and failed covers (top), and top library search result against a minerals Raman library (bottom), identifying a higher concentration of rutile (titanium dioxide) in the good cover.

Summary and conclusion

Ambient light leaking into the device caused erroneous measurements for low light level measurements. Diffuse transmission measurement of the parts by UV-Visible spectroscopy confirmed that the failed cover did not meet the specification for maximum transmittance. Thermogravimetric analysis demonstrated that the composition of the original cover contained approximately 3% more, by weight, of an inorganic filler compared to the replacement cover. Infrared ATR analysis over the mid and far-IR spectral regions showed that the original cover had significantly higher rutile (titanium dioxide) content than the replacement cover. The infrared results were confirmed by FT-Raman spectroscopy.

This study clearly shows the importance of having several tools available for root cause analysis. Many of the tools used can be found on the Nicolet iS50 FTIR Spectrometer. The Nicolet iS50 is able to collect multi-range spectra without compromise using the built-in iS50 ATR and iS50 Raman accessories. The analyses provided by the Thermo Scientific UV-Vis and FTIR instruments, along with thermogravimetric analysis, were decisive in determining the root cause failure of the plastic cover.

References

1. Thermogravimetric results provided by Jeff Jansen, The Madison Group, 2615 Research Park Drive, Madison, WI, 53711.
2. Mid-Far ATR iS50 collection program available upon request. Requires Nicolet iS50 FTIR Spectrometer configured with built-in diamond iS50 ATR, and ABX Automated Beamsplitter exchanger with KBr and solid substrate beamsplitter.
3. Thermo Scientific Application Note 50581, Advanced ATR Correction Algorithm.
4. An Infrared Spectral Library of Automobile Paint Pigments (4000–250 cm^{-1}), developed by Dr. Edward H. Suzuki at the Washington State Police Crime Laboratory, downloadable from the SWGMAT.org website
5. Downs R T (2006) The RRUFF Project: an integrated study of the chemistry, crystallography, Raman and infrared spectroscopy of minerals. Program and Abstracts of the 19th General Meeting of the International Mineralogical Association in Kobe, Japan. 003-13 Minerals 514 Raman Library.



Polymer troubleshooting guide

Polymer problems identified – simply, efficiently

Ensure raw materials, masterbatches and finished products meet your quality standards, and if not, investigate why using Thermo Scientific™ Spectroscopy Solutions.

- ✓ Thermo Scientific™ Nicolet™ Summit X FTIR Spectrometer
- ✓ Thermo Scientific™ Nicolet™ Apex FTIR Spectrometer
- ✓ Thermo Scientific™ Nicolet™ iS50 FTIR Spectrometer
- ✓ Thermo Scientific™ Everest™ Diamond ATR Accessory
- ✓ Thermo Scientific™ SMART™ iTX Diamond ATR Accessory
- ✓ Thermo Scientific™ OMNIC™ Specta™ Software
- ✓ Thermo Scientific™ OMNIC™ Paradigm Software
- ✓ Thermo Scientific™ DXR3 Raman Microscope
- ✓ Thermo Scientific™ Nicolet™ iN10 Infrared Microscope
- ✓ Thermo Scientific™ Nicolet™ iS50 Modules and Accessories

Plastic or polymer problems?

Use the Thermo Scientific™ Polymer Troubleshooting Guide to find answers.

1	Find your polymer problem	2	Learn how to analyze the problem	3	Select spectroscopy solutions to help your analysis
SYMPOTM	POSSIBLE CAUSES	SAMPLE TESTING PLAN	DATA ANALYSIS PLAN	RECOMMENDED CONFIGURATION	
What's your problem; what do you observe?	What could cause this problem?	How do you measure?	How do you identify the problem?	What to use?	
Bloom	Improper additive formulation – excess or un-reacted additive	1. Scrape material from surface 2. Measure by single-bounce ATR	1. Search libraries to identify the unknown material 2. Adjust formulation based on identified material	• Nicolet Apex FTIR Spectrometer • Smart iTX Diamond ATR Accessory • OMNIC Specta Software for Polymer Labs	
Hazing/streaking/incorrect color (white or black)	Improper formulation: additives or fillers; contamination, poor mixing	1. Measure directly or excise outer or inner material from sample 2. Measure using diamond ATR Mid-IR or Far-IR for inorganic fillers	1. Compare to reference part data and search libraries to identify differences 2. Change formulation if appropriate	• Nicolet iS50 FTIR Spectrometer • Built-in Diamond ATR Accessory • Solid-substrate beam splitter • OMNIC Specta Software for Polymer Labs	
Oily or tacky surface	Improper additive formulation or contamination	1. Wipe or scrape surface to isolate material or direct analysis 2. Measure residue or sample surface on single bounce ATR 3. Measure reference part or sample with surface cut off	1. Search libraries to identify material 2. Adjust formulation or change process to avoid contamination	• Nicolet Summit X FTIR Spectrometer • Everest Diamond ATR Accessory • OMNIC Paradigm Software with Polymer Library	
Inclusions, de-lamination, fish eyes (complex)	Poor processing, contamination	1. Isolation of included contaminants 2. Sample cross-sectioning to view layers 3. Perform microscopic analysis: a. FTIR: $\geq 5 \mu\text{m}$ b. Dispersive Raman: $\geq 1 \mu\text{m}$	1. Search libraries to identify contamination 2. Change process to avoid contamination	• Nicolet iN10 FTIR Microscope • OMNIC Specta Software for Polymer Labs OR • DXR3 Raman Microscope • OMNIC Specta Software for Raman Analytical	
Roughness, speckles, mars, bubbles	Contamination: surface or embedded processing problem (trapped gas)	1. Isolate surface or embedded material 2. Measure using single-bounce Diamond, ZnSe or Ge* ATR	1. Search libraries to identify contamination 2. Change process to avoid contamination	• Nicolet Apex FTIR Spectrometer • Smart iTX Diamond ATR Accessory • OMNIC Specta Software for Polymer Labs	
Brittle, cracking, weakness	Oxidation, degradation, contaminant, incorrect material	1. Excise surface or inner material 2. Measure by single-bounce ATR	1. Compare to reference part 2. Identify unexpected components 3. Ensure material is correct for conditions; change formulation as needed	• Nicolet Apex FTIR Spectrometer • Smart iTX Diamond ATR Accessory • OMNIC Specta Software for Polymer Labs	
Diminished physical properties	Crystallinity, structure, polymorphism, inorganic additives, degradation, contamination	Measure directly using Raman or single-bounce Diamond ATR in Far-IR range	1. Search libraries using spectral region search to identify components 2. Optimize formulation or manufacturing process	• Nicolet iS50 FTIR Spectrometer • Nicolet iS50 Raman Module • Built-in Diamond ATR Accessory • Solid-substrate beam splitter	
Material too soft or hard	Improper formulation: co-polymers, plasticizers, fillers (>1% by weight)	1. Measure directly using single-bounce Diamond, ZnSe or Ge* ATR 2. May require cutting away top surface to expose interior	1. Calculate peak height or area ratio 2. Verify co-polymer ratios 3. Adjust formulation and check ratios routinely	• Nicolet Summit X FTIR Spectrometer • Everest Diamond ATR Accessory • OMNIC Paradigm Software with Polymer Library	
	Improper formulation: low-level additives (<1% by weight)	1. Melt polymer into thin film of known thickness 2. Measure film with transmission	1. Quantify additives using peak height or area method 2. Adjust formulation 3. Check additives routinely	• Nicolet Summit X FTIR Spectrometer • Mini-Film Maker Kit	
Swelling	Surface contamination	1. Extract contamination into solvent 2. Dry onto ATR crystal or IR window 3. Measure using transmission	1. Search libraries to identify contamination 2. Determine if polymer or formulation is appropriate for application	• Nicolet Summit X FTIR Spectrometer • Everest Diamond ATR Accessory • OMNIC Paradigm Software with Polymer Library	
Warping	Improper formulation, incorrect processing conditions (if nothing found wrong with formulation)	1. Measure directly using single-bounce Diamond, ZnSe or Ge* ATR 2. May require cutting away top surface to expose interior	1. Calculate peak height or area ratio 2. Verify co-polymer ratios 3. Adjust formulation and check ratios routinely	• Nicolet Apex FTIR Spectrometer • Smart iTX Diamond ATR Accessory • OMNIC Specta Software for Polymer Labs	
Wear, premature failure	Wrong material or formulation, material failure, extreme use conditions	1. Measure directly using single-bounce Diamond, ZnSe or Ge* ATR 2. May require cutting away top surface to expose interior 3. Measure sample and reference part on TGA-IR	1. Search libraries to identify material 2. Compare sample data to reference part data to identify differences 3. Change formulation if appropriate	• Nicolet iS50 FTIR Spectrometer • Built-in Diamond ATR Accessory • TGA Interface Module • OMNIC Specta Vapor Phase library	
Odor	Oxidation, degradation, contamination	1. Solvent extraction, evaporate solvent 2. Measure residue on ATR or IR window 3. Measure sample and reference part on TGA-IR	1. Search libraries to identify material or contamination 2. Compare sample data to reference part data to identify differences 3. Change formulation if appropriate	• Nicolet Apex FTIR Spectrometer • TGA Interface Module • OMNIC Specta Vapor Phase library	
Need to verify raw materials	Inconsistent or out-of-specification bulk ingredients (>1% by weight)	1. Measure directly using single-bounce ATR OR 2. Measure polymer beads on NIR integrating sphere Sample Spinner or powders in containers by NIR Fiber Probe	1. Use QCheck function to correlate spectrum with reference material OR 2. Use chemometrics model to identify and quantify ingredients 3. Apply statistical process control to ensure product consistency	• Nicolet Summit X FTIR Spectrometer • Everest Diamond ATR Accessory OR • Nicolet iS50 FTIR Spectrometer • Nicolet iS50 NIR Module	
	Inconsistent or out-of-specification low-level ingredients (<1% by weight)	1. Melt polymer into thin film of known thickness 2. Measure film with transmission	1. Quantify additives using peak height or area method 2. Apply statistical process control to ensure product consistency	• Nicolet Summit X FTIR Spectrometer • Mini-Film Maker Kit	

* Ge for Carbon-filled polymers • TGA-IR = Thermogravimetric Analysis Infrared; NIR = Near infrared; FTIR = Fourier transform infrared; ATR = Attenuated total reflectance.

Watch how-to videos and download application notes from our Polymer Resource Center at thermofisher.com/polymeranalysis

Product selection guide

Spectroscopy solution by task and sample property



Polymer analysis kits

We offer kits that combine commonly used tools for polymer analysis. They include our patented Multi-Component Search, a 13,000 compound spectral library and 240-page Infrared Spectroscopy of Polymers Knowledgebase along with appropriate sampling device(s). For more details, see the FTIR Polymer Analysis Kit flyer (FL52273_E).

Using the table below, find your task and sample feature to select the instrument configuration and solve your polymer problems.

Thermo Scientific™ instruments	Task	QA/QC verification			Material characterization			
		Property	Component concentration >1%	Component concentration <1%	Bulk	Physical/chemical formulation	Fillers, inorganic pigments	Crystallinity, morphology
Nicolet Summit X FTIR Spectrometer	Everest Diamond ATR* Accessory	Hot-pressed Film Kit						
Nicolet Apex FTIR Spectrometer	Smart iTX ATR Accessory	Hot-pressed Film Kit	Smart NIR Integrating Sphere	In-compartment TGA accessory + Mercury TGA Software				
Nicolet iS50 FTIR Spectrometer	Built-in Diamond ATR* or Smart iTX ATR Accessory	Hot-pressed Film Kit	iS50 NIR Module	TGA-IR accessory + Mercury TGA Software	Built-in Diamond ATR + Solid Substrate beamsplitter	iS50 Raman Module		
Nicolet iN10 Microscope	Micro Tip ATR* accessory	Hot-pressed Film Kit		Nicolet iZ10 Module + In-compartment TGA accessory + Mercury TGA Software				Nicolet iN10 Infrared Microscope
DXR3 Raman Microscope					DXR3 Raman Microscope	DXR3 Raman Microscope	DXR3 Raman Microscope	

* ATR is a useful tool for quick, basic material and additives characterization



Nicolet Summit X FTIR Spectrometer with Everest ATR Accessory



Nicolet Apex FTIR Spectrometer with iTX ATR Accessory



Nicolet iS50 FTIR Spectrometer with TGA-IR accessory



DXR3 Raman Microscope or Nicolet iN10 Microscope



For small particle identification and polymer characterization that requires high-spatial resolution

For streamlined QA/QC testing of polymers and ingredients

For high-performance polymer QA/QC and contaminant/failure analysis

For polymer method development, deformulaion, troubleshooting and research



Characterization of contaminants in recycled PET and HDPE using FTIR microscopy

Authors

Suja Sukumaran, PhD,
and Rui Chen, PhD,
Thermo Fisher Scientific

Introduction

Reducing environmental pollution and energy consumption in recycling are the paramount driving forces behind research on recycling plastics. The advances in reclamation technologies have pushed the boundaries of recycled plastics or post-consumer resin (PCR) use to include many high-end applications such as food packaging, electronics, and automobiles. These applications often demand near-prime qualities of any recycled plastics. Furthermore, as more and more countries across the globe ban the use of single use plastics, there has been a steady increase in the demand for PCR over virgin resins. To ensure the performance and aesthetic quality of recyclates in second-market applications, it is imperative that fast, reliable, and cost-effective characterization and quality control procedures are implemented at different stages of recycling and manufacturing operations.¹

The challenges in large-scale use of recyclates in the second-market plastic manufacturing arise from the unknown origins of the feedstock, the presence of any contaminants, and possible degradation during previous usage. Traditionally, bulk properties such as melt flow rate and mechanical properties have been used to assess the quality of the recyclates. These macroscopic properties, however, are only indirectly correlated to materials' underlying chemistry and cannot identify contaminants. To that end, FTIR microscopy can provide a more holistic understanding of the material at molecular level by annotating sample morphology with chemical information.

In this application note, we demonstrate the use of FTIR microscopy for the characterization of recycled polyethylene terephthalate (PET) and polyethylene (PE) PCRs. The results show that cellulosic fragments are common contaminants in recycled polymers. Depending on the morphology of the contaminants, different sampling techniques should be adopted for the analysis.

Materials and methods

FTIR microscopy was carried out using a Thermo Scientific™ Nicolet™ iN10 MX Infrared Imaging Microscope. Three modes of analysis were used: reflection, transmission and micro ATR (μ -ATR). These were applied across different types of sample sets.

For the PET powder sample, an area map was collected in reflectance mode. The PET powders were spread onto a gold slide and analyzed without further sample preparation. The XY area map was collected using an MCT-A detector, 50 μ m spatial resolution, and 8 scans at 8 cm^{-1} spectral resolution at each map point.

For the analysis of the PE pellets, particles were first isolated from the surface of the pellets under a preparatory microscope at 3 \times magnification. Isolated particles were then placed onto a glass slide and analyzed in ATR mode. A slide-on germanium (Ge) tip ATR was used for the analysis of the isolated contaminant particles. An MCT-A detector was used for all samples, and 64 scans at 4 cm^{-1} resolution were collected in 22 seconds for each spectrum. The Ge crystal tip was cleaned between sample analyses using 70% isopropanol.

A grocery bag sample was analyzed as received. A small piece of the grocery bag sample was cut, placed on a transmission holder, and analyzed in transmission mode. An area map with a spatial resolution of 50 μ m was collected, using 4 scans at 8 cm^{-1} spectral resolution at each XY map point.

Results and discussion

Characterization of recycled PET powders by reflectance FTIR microscopy

Polyethylene terephthalate (PET) accounts for approximately 10% of the plastic produced worldwide and is extensively used for single use bottle packaging. Figure 1 summarizes the reflectance FTIR microscopy experiments of the recycled PET powders. An area of approximately 2.5 \times 2.5 mm 2 was mapped, in which the PET particles range from tens to hundreds of micrometers in dimension. There are noticeable fibrous features in the optical image (Figure 1A). The FTIR spectrum of the particles (Figure 1C) shows a positive match to PET. The PET spectrum was then used as the reference spectrum for correlation profiling, and the resulting correlation map was superimposed with the optical image (Figure 1B); the warm color indicates a high degree of correlation. Major peaks characteristic to PET, such as 1710 cm^{-1} (the C=O stretching), 1241 cm^{-1} and 1094 cm^{-1} (the C-O stretching), 844 cm^{-1} (trans CH₂ rocking) and 723 cm^{-1} (the aromatic C-H out-of-plane bending), are observed in both the sample spectrum (red) and reference spectrum (blue). Note that the peak at 3430 cm^{-1} , attributed to the hydroxyl groups, shows a higher relative intensity in the recycled PET. The chain scissions during PET recycling could generate polymer radicals with hydroxyl groups.²

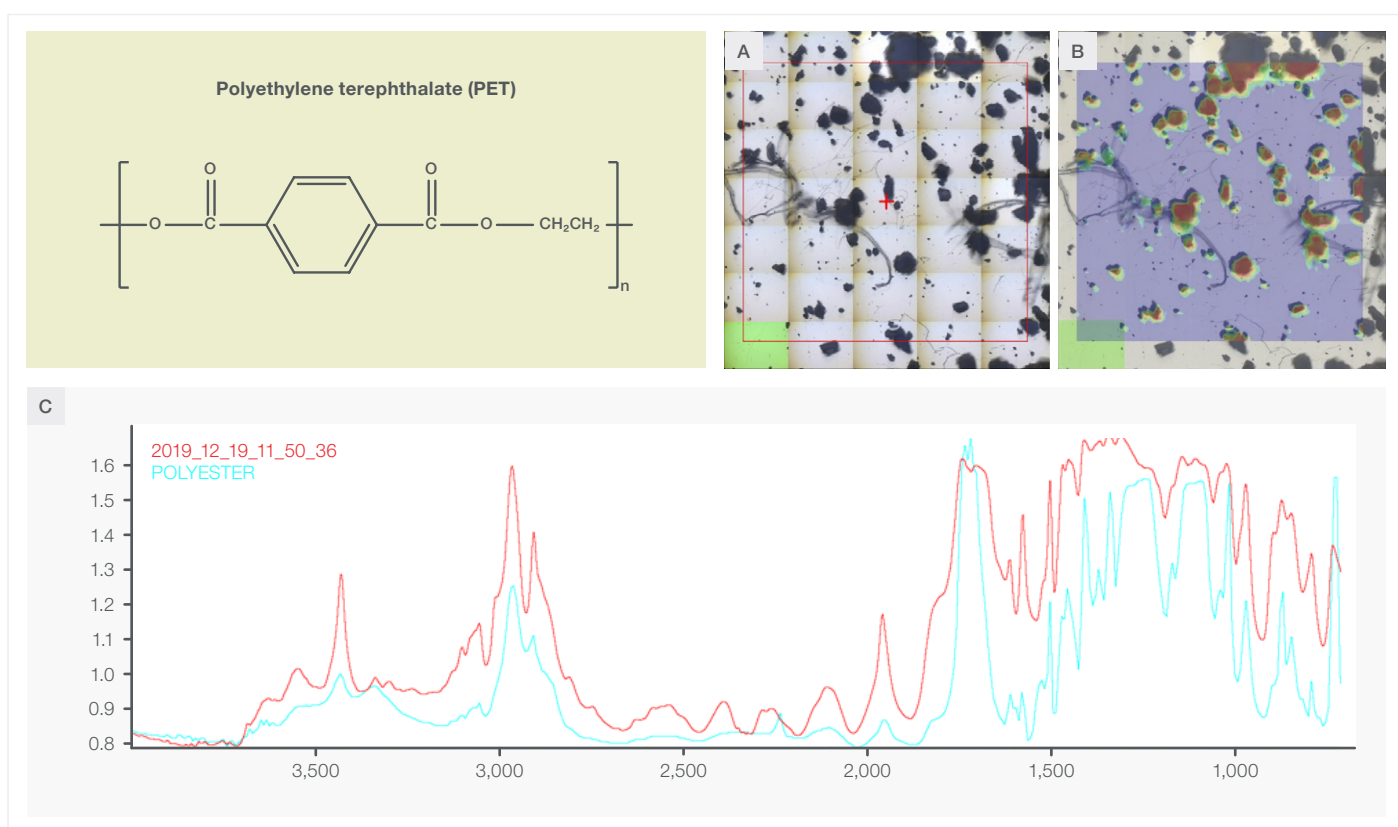


Figure 1. Analysis of recycled PET powders using reflectance FTIR microscopy. (A) Optical image of the recycled PET powders spread on a gold slide. (B) Chemical image superimposed with the optical image. The chemical image is the correlation profile using the PET spectrum as the reference. (C) Reflectance FTIR spectra of the recycled PET particles (red) and the standard reference spectrum from the library (blue).

The same procedure was repeated for the fibrous features observed in the optical image (Figure 2A). The resulting spectrum (Figure 2C) shows a positive match to cellulose. The observed peaks in the spectral range of 3600 - 2900 cm⁻¹ are characteristic for the stretching vibrations of the O-H and C-H bonds in polysaccharides: the band at ~2900 cm⁻¹ is attributed to the C-H stretching vibration of the hydrocarbon constituent, and the broad peak centered at 3300 cm⁻¹ is ascribed to the stretching vibration of the hydroxyl group, including both inter- and intra-molecular hydrogen bond vibrations. In the fingerprint region, the peaks located at ~1640 cm⁻¹ correspond to the vibration of water molecules absorbed in cellulose. The absorption bands at 1428, 1367, 1334, 1027 and 896 cm⁻¹ arise from stretching and bending vibrations of -CH₂ and -CH, -OH and C-O bonds in cellulose.³ Cellulose is mainly used to produce paperboard and paper and therefore it is a common contaminant found in recycled polymers, possibly originating from labels and stickers on many consumer products. Cellulosic contaminants are undesirable as they can be cascaded into the end products, negatively affecting the products' performance and aesthetic.

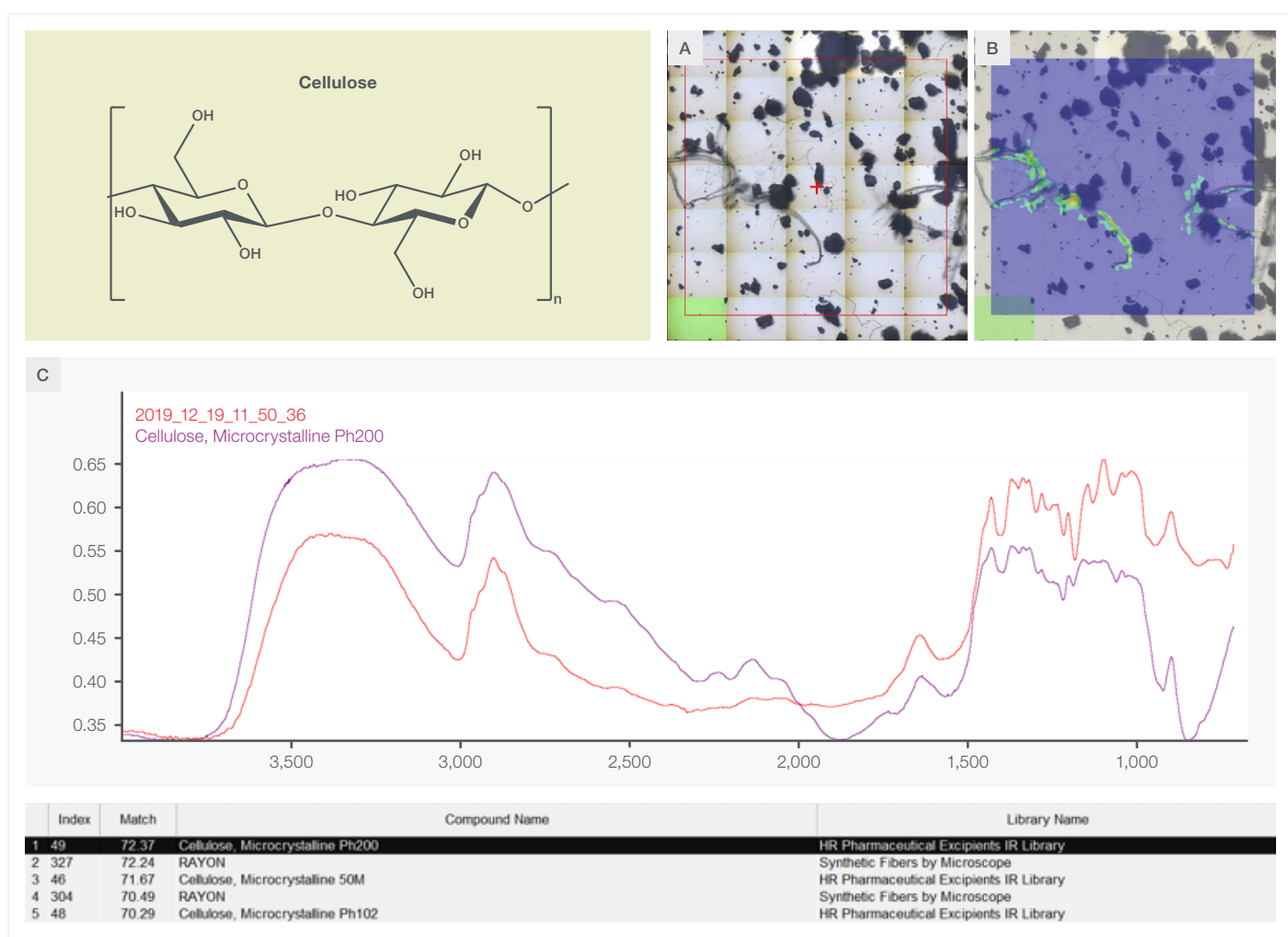


Figure 2. Analysis of the fibers in the recycled PET powders using reflectance FTIR microscopy. (A) Optical image of the recycled PET powders spread on a gold slide. (B) Chemical image superimposed with the optical image. The chemical image is the correlation profile using the cellulose spectrum as the reference. (C) Reflectance FTIR spectrum of the cellulose fibers (red) and the standard reference spectrum from the library (purple).

Analysis of the contaminants in recycled HDPE pellets by ATR FTIR microscopy

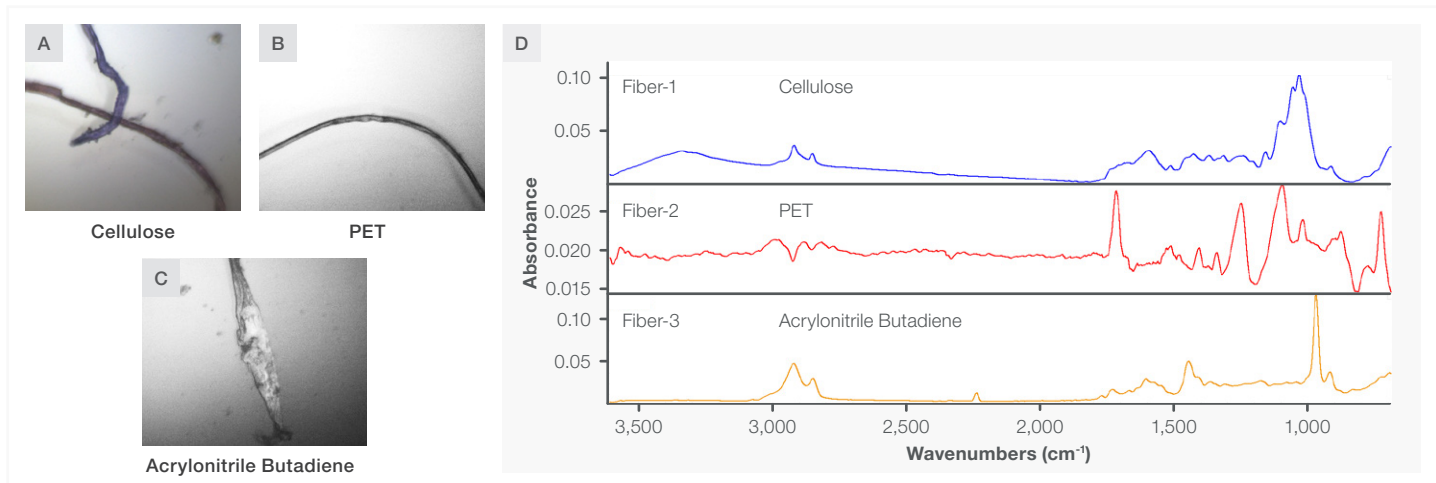


Figure 3. μ -ATR FTIR microscopy of recycled PE pellets.

The FTIR microscopic analysis shows that there are at least three types of fibers present in the recycled HDPE pellets: cellulose (Figure 3A), PET (Figure 3B) and acrylonitrile butadiene (Figure 3C). The representative FTIR spectra of the three types of fibers are shown in Figure 3D, where the fibers can be readily differentiated.

In the same pellet sample, there are visually discernible black particles (insert of Figure 4). The particles were isolated from the pellet and subjected to μ -ATR FTIR microscopy analysis. The results are shown in Figure 4. Upon library search, the particles show a match to cellulose but with a low matching value. Most likely, these particles are charred cellulose. There are pronounced differences in FTIR spectra across the whole spectral range between cellulose and the particles. In particular, the peaks associated with the O-H group, such as those at $3600\text{-}3100\text{ cm}^{-1}$ (stretching vibration of the hydrogen bonded O-H in polysaccharides), $1630\text{-}1650\text{ cm}^{-1}$ (the O-H bending from the water molecules absorbed in cellulose), and 2940 and 2860 cm^{-1} (asymmetric and symmetric stretching vibrations of the C-H hydroxyl groups), are either absent or present at much lower intensities, suggesting the dehydration reactions during the cellulose \rightarrow charred cellulose transformation. In addition, the peak at $\sim 900\text{ cm}^{-1}$, which is attributed to β -glycosidic linkage between glucose units, is absent, suggesting the breakage of the pyranose linkage in cellulose. The peaks associated with the pyranose, such as those at 1428 cm^{-1} and 1370 cm^{-1} (CH_2 and CH bending of pyranose ring), and 1034 cm^{-1} (C-O-C pyranose ring vibration), are preserved but with decreased intensity^{4,5}.

It should be noted that μ -ATR often provides the best S/N for the resulting spectrum, which lends itself to library searching. In addition, it requires little to no sample preparation, whereas other modes of analysis often involve sample preparation steps such as flattening the samples for reflectance analysis or compressing the samples into thin sections for transmission analysis.

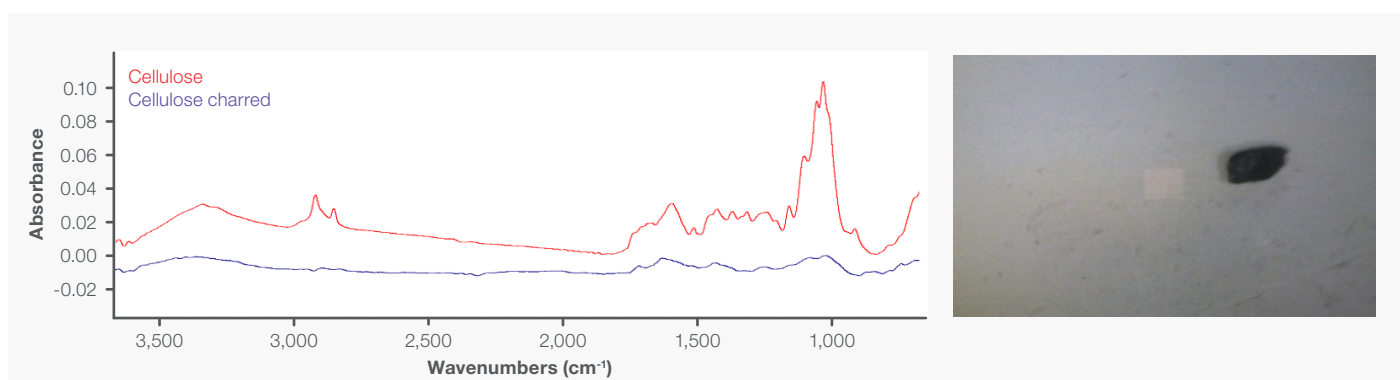


Figure 4. ATR FTIR spectrum of a black particle in the recycled PE pellets.

Analysis of the particles present in grocery bags by transmission FTIR microscopy

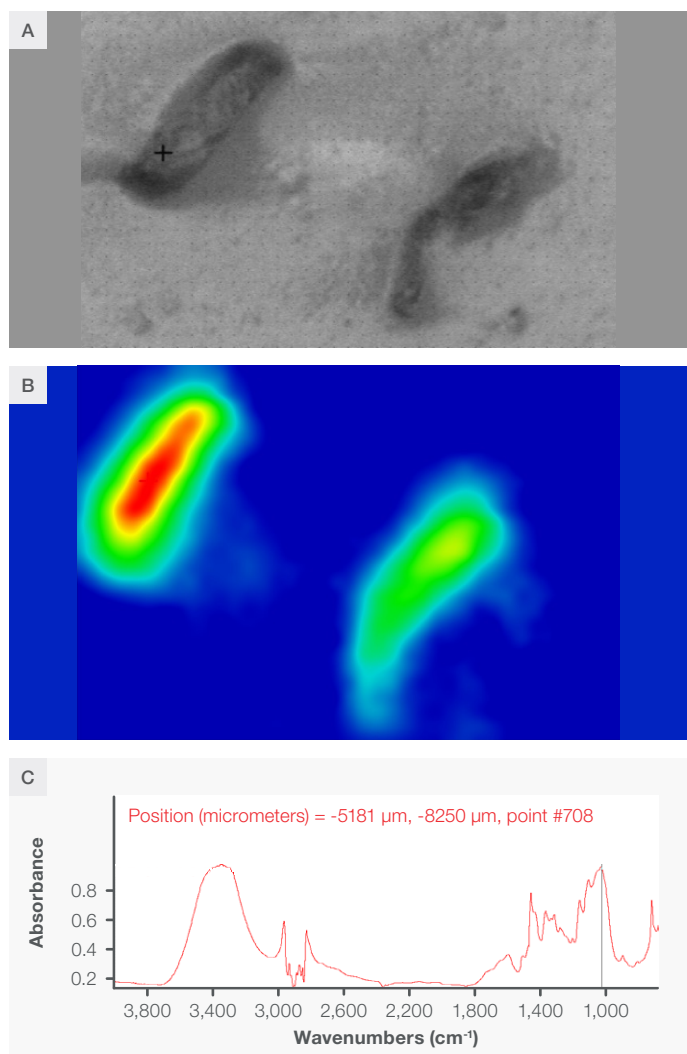


Figure 5. Transmission FTIR microscopy of grocery bag made from recycled LDPE. (A) Optical image of a piece of grocery bag showing two particles embedded in the sample matrix. (B) Chemical map of the sample constructed using cellulose spectrum as the reference. (C) FTIR spectrum of the grocery bag sample with PE spectrum subtracted.

The grocery bag was made out of recycled LDPE. A small piece was cut and analyzed in the transmission mode with no further sample preparation. Two particles were located (Figure 5A). Due to the thickness of the film, the peaks are saturated. In order to extract the spectrum of the contaminant particles, the PE peaks were subtracted from the total spectrum and the resulting spectrum is shown in Figure 5C. The ensuing search shows a match to cellulose. Correlation profiling using the cellulose spectrum results in the chemical image shown in Figure 5B.

Conclusions

In this application note, FTIR microscopy was successfully applied for the analyses of the contaminants found in recycled polymers. In all samples analyzed, cellulose, in either its native or charred form, was identified as a contaminant. The comparison between cellulose and charred cellulose provides an insight to the difference in their underlying chemistry, which can be beneficial for understanding the origins of the contaminants as well as their associated recycling processes. Additional fibrous contaminants, PET, and acrylonitrile butadiene, were identified in the recycled HDPE pellets, illustrating the chemical specificity of FTIR microscopy. Three sampling modes—reflectance, μ -ATR, and transmission—were used for the analyses, demonstrating the flexibility and versatility of FTIR microscopy to suite different sample types.

References

1. Francisco Vilaplana, Sigbritt Karlsson, Quality Concepts for the Improved Use of Recycled Polymeric Materials: A Review, *Mater. Eng.* 2008, 293, 274–297
2. Bina Bhattacharai, Yukihiko Kusano, Tommy Licht Cederberg, Lisbeth Krüger Jensen, Kit Granby, Gitte Alsing Pedersen, Chemical characterization of virgin and recycled polyethylene terephthalate films used for food contact applications, *European Food Research and Technology* (2024) 250:533–545.
3. Viola Hospodarova, Eva Singovszka, Nadezda Stevulova, Characterization of Cellulosic Fibers by FTIR Spectroscopy for Their Further Implementation to Building Materials, *American Journal of Analytical Chemistry*, 2018, 9, 303–310.
4. Ivana Pastorova, Robert E. Botto, Peter W. Arisz, Jaap J. Boon, Cellulose char structure: a combined analytical Py-GC-MS, FTIR, and NMR study, *Carbohydrate Research*, 1994, 262 (1), 27–47.
5. Nicole Labbe, David Harper, Timothy Rials, Chemical Structure of Wood Charcoal by Infrared Spectroscopy and Multivariate Analysis, *Agric. Food Chem.* 2006, 54, 3492–3497.

Sampling considerations for the measurement of a UV stabilizer in polymer pellets using FT-NIR spectroscopy

Keywords

Antaris, additives, FT-NIR, polymer, polystyrene, sample cup, spinner

Abstract

For heterogeneous samples such as polymer pellets, it is critical to obtain a measurement that is representative of the bulk sample rather than a small fraction of the material. This is often a significant challenge when using traditional near-infrared spectroscopy sampling methods. Accessories such as the Sample Cup Spinner allow a greater amount of material to be analyzed in an automated device. In this study, two diffuse reflectance-sampling methods were compared to determine the most efficient and accurate method for sampling polystyrene pellets. A single calibration model was developed to determine the concentration of an ultraviolet (UV) stabilizer additive in polystyrene pellets. Using the two sampling methods, the concentrations of four unknown samples were determined using the single model. The results demonstrate that the Sample Cup Spinner accessory provides the optimum performance with the shortest analysis time.

Introduction

With the high production rates in the polymer industry, it is essential that a quick, accurate, and easy-to-use analytical technique is available to monitor the quality of the material produced. Traditional methods, such as titration or extraction followed by GC, require sample preparation by a trained technician and often deliver results to the production personnel after a significant time lapse. This time lag between sampling and the completion of the analysis can produce out-of-specification material, resulting in manufacturing inefficiency, high scrap levels, and the need to rework product that does not meet quality standards.

Fourier transform near-infrared (FT-NIR) is an ideal tool for at-line or near-line quality control analysis of polymer pellets. It offers several advantages over traditional quality control techniques, including:

- Availability of answers in minutes allowing faster feedback to the production personnel and improvement of process efficiency
- Ability to perform analyses at-line
- No sample preparation
- Elimination of the need for purchase and disposal of hazardous reagents
- Improved operator-to-operator reproducibility
- Reduced cost of quality control testing
- Non-destructive testing making the samples available for analysis by other techniques



Figure 1. Sample Cup Spinner for the Thermo Scientific™ Antaris™ FT-NIR analyzer.

For heterogeneous materials such as polymer pellets, a small sample may not be representative of the bulk material. Each pellet or group of pellets may have a slightly different composition than the next. For this reason, a representative sampling method is needed. This is often achieved by the use of a cup with a quartz window. The sample cup provides a way to analyze greater amounts of material without having to empty the first sample and replace it with a new sample from the same batch. Once the sample is placed in the cup, it can be analyzed by two methods.

1. Using the Sample Cup Spinner accessory (Figure 1), the sample can be rotated, constantly exposing new sample to the incident beam during data collection. A single spectrum is obtained that is representative of the material in the cup. The Sample Cup Spinner allows the largest volume of material to be analyzed in a single measurement..

Experimental

A set of 17 polystyrene pellet samples were obtained from a proprietary source. The concentration of a UV-stabilizing additive ranged from 42% to 58% by weight. The pellet shapes and sizes varied slightly from sample to sample. The samples were placed into the open powder sampling cup, which has a 47.8 mm quartz window, and analyzed by diffuse reflectance using the Integrating Sphere Module of the Thermo Scientific™ Antaris™ FT-NIR analyzer (Figure 2).



Figure 2. Antaris FT-NIR Solid Sampling system with Sample Cup Spinner.

The analyzer's Integrating Sphere Module provides a highly efficient method for collecting diffuse reflectance data for solid samples such as polymer pellets. A background was collected for each sample using the internal gold reference of the integrating sphere. The internal reference allows the background to be collected even if the sample cup is in place. Using Thermo Scientific™ RESULT™ data collection software, all spectra were acquired at 8 cm^{-1} resolution and 16 scans with a collection time of less than 10 seconds. Spectra used to develop the method were obtained using the Sample Cup Spinner accessory. The Sample Cup Spinner was adjusted so

that the largest amount of sample possible passed through the NIR beam in one complete revolution. Thirteen of the samples were used to develop the FT-NIR model and four samples were used to validate the performance of the model using the two sampling methods.

Once the model was developed, the validation samples were analyzed and the concentration of the additive was determined 30 times each using the Sample Cup Spinner and the manual single point measurement technique. To accomplish the manual single point analysis, the sample was manually rotated approximately 40 degrees between each successive measurement.

The Thermo Scientific™ TQ Analyst™ quantitative analysis software was used for all chemometric modeling. A cross-validation using a leave-one-out protocol was used to confirm the results obtained for the calibration.

Results and discussion

One spectrum was collected for each of the samples in the calibration set (13 samples total) using the Sample Cup Spinner accessory (Figure 3).

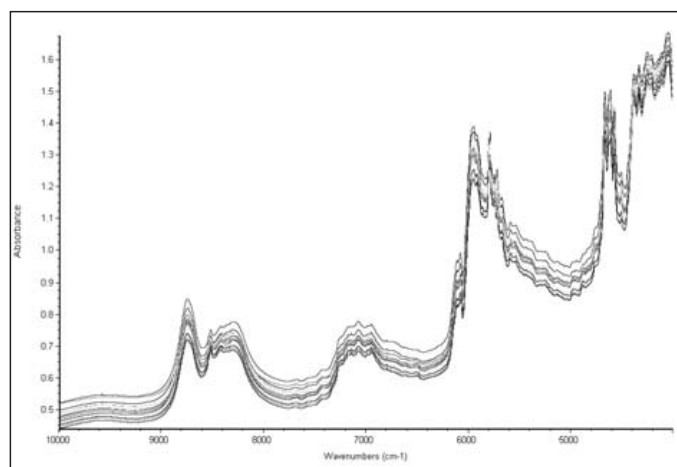


Figure 3. Calibration spectra obtained using the Sample Cup Spinner.

The total analysis time for each sample was about 15 seconds. The second derivative spectra of the calibration samples were used to develop the chemometric model (Figure 4).

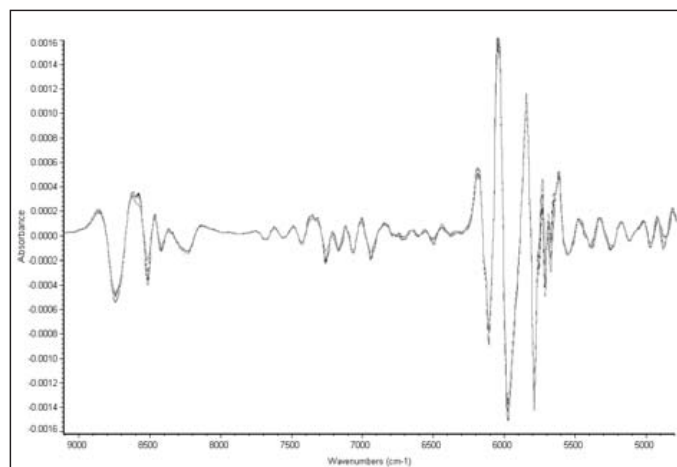


Figure 4. Second derivative spectra.

A Norris second derivative (5 segment, 0 gap) was used to pre-treat the data. A two-term Stepwise Multiple Linear Regression (SMLR) model was constructed. Using data points of 7332 cm^{-1} and 5091 cm^{-1} , a correlation coefficient of 0.9995 and RMSEC of 0.147 weight % were obtained (Figure 5). The first data point (7332 cm^{-1}) of the SMLR calibration is in the first overtone region and the second point at 5091 cm^{-1} is in the combination band region. A cross-validation using the leave-one-out protocol gave an RMSECV of 0.179 weight %.

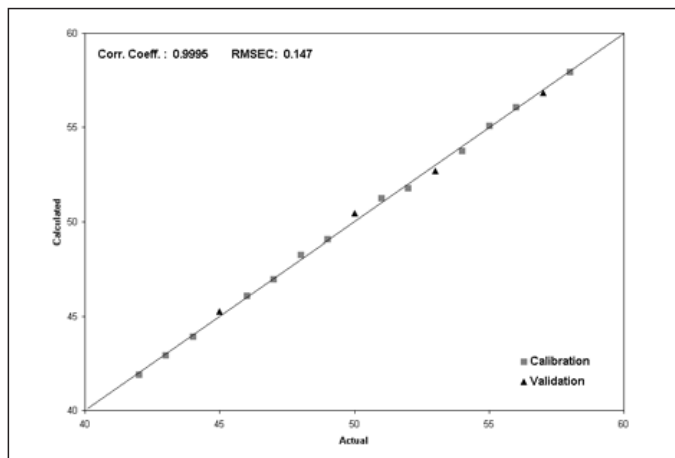


Figure 5. Calibration results using the Sample Cup Spinner.

The additive concentration in the validation samples was determined using the SMLR model. The RMSEP (Root Mean Square Error of Prediction) was 0.302 weight % for the samples analyzed using the Sample Cup Spinner. The results obtained using the Sample Cup Spinner and the manual single point measurement techniques were compared. The spectra obtained using the Sample Cup Spinner and the single point measurements are shown in Figures 6 and 7, respectively. Upon visual inspection, the spectra collected using the Sample Cup Spinner are more reproducible than those collected using the single point sampling method. The variability seen with the single point measurement method is expected because each spectrum represents only a fraction of the sample and does not account for the heterogeneity of the material. The Sample Cup Spinner continuously rotates multiple areas of the cup through the NIR beam, therefore the single spectrum that is obtained better represents the bulk of the material.

Comparison of the standard deviation of the predicted values obtained using the Sample Cup Spinner and the single point manual measurements clearly demonstrates that the Sample Cup Spinner is more reproducible and more accurately predicts the additive concentration in the validation sample (Table 1). The standard deviation of the results obtained using the single point measurement technique is two times more than that obtained using the Sample Cup Spinner. The variability in the results between the two sampling techniques for the 30 measurements is presented graphically in Figure 8.

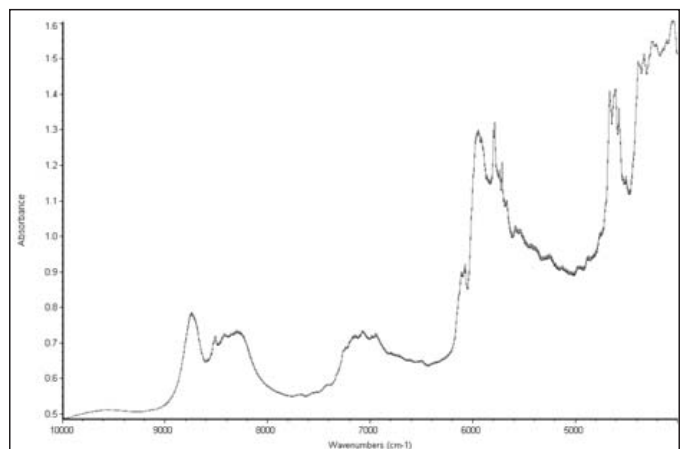


Figure 6. Spectra of unknown sample obtained using Sample Cup Spinner.

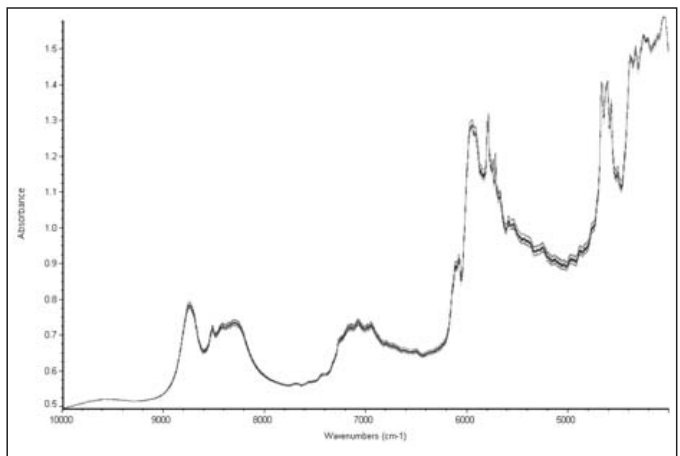


Figure 7. Spectra of unknown sample obtained using single point measurement method.

	Expected value	Sample cup spinner	Single point measurement
Validation sample 1	57	56.84	55.78
Validation sample 2	53	52.69	51.97
Validation sample 3	45	45.26	44.52
Validation sample 4	50	49.33	49.08
Standard deviation – validation sample 4		0.29	0.62
% Relative standard deviation – validation sample 4		0.29	1.27
Range – validation sample 4		1.18	2.44

Table 1. Prediction results for additive concentration (weight %).

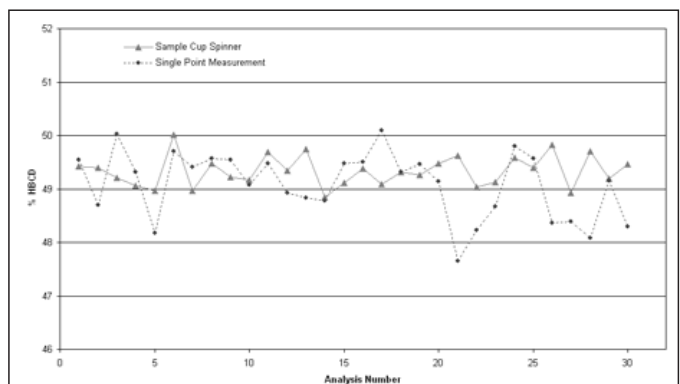


Figure 8. Variability of Sample Cup Spinner results versus single point measurement for sample 1.

Conclusions

The Antaris FT-NIR analyzer offers an excellent alternative to traditional methods for determination of additive levels in polystyrene. The main advantage of FT-NIR spectroscopy is that production efficiency is enhanced due to the quicker availability of reliable data. The use of the Sample Cup Spinner reduces the analysis time. By allowing a greater volume of sample to be analyzed, the Sample Cup Spinner provides more representative information on a heterogeneous sample and eliminates the need to analyze multiple samples from the same lot to obtain a representative result.

The data were collected using an older model instrument Antaris FT-NIR. Currently, Thermo Fisher Scientific offers an improved model, the Antaris II FT-NIR, which offers superior speed and performance over its predecessor model.

Notes

Learn more at thermofisher.com/polymeranalysis

thermo scientific

For research use only. Not for use in diagnostic procedures. For current certifications, visit thermofisher.com/certifications
© 2026 Thermo Fisher Scientific Inc. All rights reserved. All trademarks are the property of Thermo Fisher Scientific and its subsidiaries unless otherwise specified. **MCS-CM1641-EN 01/26**